Numerical Investigation of Thermal Radiation and Activation Energy Effects on MHD Mixed Squeezing Flow of $Cu–Al_2O_3–Ag$/EG Ternary Nanofluid in a Rotating Channel with Non-Uniform Heat Sources

H.G. Suguna[1], B. Sreenivasa Reddy[2]

[1]Associate Professor, Department of Mathematics, GFGC, Sidlaghatta, Chikkaballapur (Dt), Karnataka, India
[2]Professor, Department of Applied Mathematics, Yogi Vemana University, Kadapa, A.P., India.

Abstract
The Present research paper an attempt the MHD mixed squeezing flow of a $Cu–Al_2O_3–Ag$/ethylene-glycol ternary nanofluid in a rotating channel is examined in this work under the combined impacts of activation energy, thermal radiation, and non-uniform heat sources. Magnetic-field effects, rotational motion, radiative heat transmission, irregular heat generation, and temperature-dependent chemical reactions are all included in the formulation of the governing nonlinear momentum, energy, and concentration equations. The governing equations are reduced to set of ordinary differential equations and then numerically solved by employing Runge-Kutta-Fehlberg fourth-fifth order method. Effect of pertinent parameters on velocity, temperature and nano-concentration fields is examined through the plots. Skin-friction coefficients, Nusselt number and Sherwood number for different variations are studied numerically. The authors have hope that the results obtained in the present study not only provide useful information for applications, it also serves as a complement to the previous studies.

Keywords: Squeezing flow; $Cu–Al_2O_3–Ag$/Eg ternary nanofluid; thermal radiation; activation energy; heat source; heat and mass transfer.

1. Introduction

Pure fluids such as oil, ethylene glycol, and water have less thermal conductance which is a constraint in the flow phenomenon of the fluid. For improving the thermal conductivity of base/pure fluid, scientists have introduced different techniques and methods. One of such technique is the suspension of small sized particles, introduced first by Choi and Eastman [6]. Sheikholeslami and Ganji [65] have discussed water-based copper nanofluid flow through two squeezing plates. The authors of this study have determined the viscosity and thermal conductivity of nanoparticles by employing Brinkman and Garnetts model with a fine agreement with other results in literature. It has concluded in this work that the thermal conductance of the fluid has been controlled by the extending values of Eckert number and volumetric fraction of nanoparticles. Nanofluid flow reduces [4, 8, 10, 12, 14, 23, 40, 53, 59, 78] the resistance to heat transfer for different flow systems.

With the passage of time, researchers came to know that the spread of two different types of nanoparticles in a pure fluid further augments the thermal flow characteristics. (ey termed such fluid as a hybrid nanofluid. Lund et al. [38] have inspected the dynamics of hybrid nanofluid flow with influence of thermal radiations and viscous dissipation past a stretching surface and have determined two branches of solutions. It has observed by the authors that the upper branch of solution has highlighted to be more applicable due to its stable nature. Khan et al. [Khan et al.[31, 32], Waseem et al [81] have deliberated an incredible work todiscuss the thermal flow improvement for hybrid nanofluid flow by means of different flow geometries and flow conditions.

In recent years, three dissimilar kinds of nanoparticles were suspended in a pure fluid, by scientists and experimenters, in order to construct an unexplored category of nanofluids: 'ternary hybrid nanofluid' was the name given to this novel category of nanofluids. Specialists were driven to change the existing nanofluids as a result of the increased demand for cooling substances combined with great thermal potential at the industrial level: this need led to the introduction of a trihybrid nanofluid with the specified thermal properties. The behaviors of the trihybrid nanofluid ($TiO2+CuO+MgO/H_2O$) were addressed by Mousavi et al. [32]. To increase the viscosity of the trihybrid nanofluid, Sahoo et al. [57] attempted to promote a novel correlation.

About ten years ago, Choi [6] suggested using suspended nanoparticles in a base fluid to boost heat conductivity. Since then, Wang et al. [40], Eastman et al. [9], Buongiorno [5], and others have carried out theoretical and experimental studies on the nanofluid heat transfer property. They have come to the conclusion that the addition of nanoparticles can significantly increase the base fluid's thermal conductivity. Additionally, two models—the single-phase model and the two-phase model—are provided to integrate the influence of nanoparticles on fluid flow issues. The Buongiorno model addresses two significant mechanisms: thermophoresis and Brownian motion.

Numerous writers, including Hamad and Pop [18], Kuznetsov and Nield [36], and Sheikholeslami and Ganji [66]. In a rotating frame of reference, Turkyilmazoglu and Pop [72], Das [9] investigated the effects of MHD on nanofluid flow in a permeable channel past a vertical infinite plate with thermal radiation, a constant heat source, and a convective boundary condition. The heat and mass transfer behaviour of an unstable nanofluid flow between parallel plates in the presence of thermal radiation has been reported by Sheikholeslami and Ganji [67]. They get to the conclusion that when the radiation parameter rises, solutal boundary layer thickness increases as well.

Heat and mass transfer in several industrial and technical applications are the result of buoyancy effects brought on by chemical species and thermal diffusion. In order to improve a wide range of technologies, including underground energy transportation, the production of polymers and ceramics, enhanced oil recovery, food processing, fog formation and dispersion, temperature and moisture distribution across environmental pollution, agricultural fields and it is helpful to study the conjugate effects of heat and mass transfer. There are several uses for the heat and mass transfer flow of an electrically conducting fluid in the presence of a transverse magnetic field, including metallurgical industries, nuclear reactors, accelerators, pumps, flow metres, and MHD generators. Numerous real-world applications in astrophysical and geophysical contexts further demonstrate its applicability.

Biomechanics, artery flow, food processing, polymer processing, compression, injection modelling, and mechanical, industrial, and chemical engineering are just a few of the engineering and industrial processes where squeeze flow shows promise. In many hydrodynamical machineries and instruments, squeeze flows are often produced when normal loads or vertical velocities are applied because of moving boundaries. In order to begin the analysis, Stefan [69] took into account the squeezing flow of a Newtonian fluid with lubrication assumption. The groundbreaking work of Stefan [69] for flow between two parallel discs was expanded by Leider and Bird [37] and Hamza [19]. An electrically conducting fluid between two parallel discs, with the bottom disc being permeable and the top disc impermeable, was thoroughly analysed by Domairry and Aziz [13]. Several Authors have (Joneidi et al.[29], Hayat et al.[25] Domairry and Aziz [13] Hussain et al. [27] Shaban et al.[60]) analyzed the effects of suction/injection and squeeze Reynolds number on the magnetohydrodynamic flow between two parallel disks to second-grade fluid using HAM homotopy analysis method.

On the other hand, an unsteady squeezing flow of an electrically conducting fluid occurs in many engineering and industrial applications such as lubrication, food industries, transient loading of mechanical components, power transmission, polymer processing, compression and injection modelling. The squeezing flow of a fluid was first introduces by Stefan [69], Following this work, many researchers have investigated such flow with different aspects. Numerical solution for a fluid film squeezed between two parallel plane surfaces, mixed convection three-dimensional squeezing flow of an incompressible Newtonian fluid between two vertical parallel planes with rotating channel have been reported by Hayat et al [24], Mahanthesh et al [39], Munawar et al [44], Mustafa et al [45], have studied mixed MHD convection squeezing three-dimensional flow in a rotating channel filled with nanofluid. Das [9] have found that the volume fraction parameter decreases the rate of heat transfer in a fully developed mixed convection flow through a vertical channel filled with water based nanofluid with the uniform transverse magnetic field. Freidoonimehr et al. [15] presented the analytical solution for three-dimensional squeezing nanofluid flow in a rotating channel using Tiwari and Das model. With the aid of same model Gireesha et al. [16] have studied the effect of nanoparticles on flow and heat transfer of dusty fluid.A numerical study for the three-dimensional squeezing flow of nanofluid in a rotating channel with a lower stretching wall suspended by carbon nanotubes was further examined by Umar Khan et al. [73]. The FDM analysis for squeezed flow of a hybrid nanofluid with Cattaneo-Christov (C-C) heat flux and convective boundary condition has been examined by Khursheed Muhammad et al. [34]. Unsteady Squeezing Flow of Carbon Nanotubes with Convective Boundary Conditions was covered by Hayat et al. [20]. The unstable squeezing flow of a Cu-Al2O3/water hybrid nanofluid in a horizontal channel with a magnetic field has been studied by Najiyah Safwa Khashi et al. [47]. Using the Keller box technique, Mohib Hussain et al. [42] have examined an effective heat transfer study of MHD flow of a hybrid nanofluid between two vertically rotating plates. The mixed convection squeezing flow of nanofluids in a rotating channel with heat radiation has been studied by Wankui Bu et al. [76]. The entropy generation and statistical analysis of MHD hybrid nanofluid unstable squeezing flow between two parallel rotating plates with activation energy were done numerically by Nimer Murshid et al. [48].

Researchers have recently discovered that the thermal conductivity of a pure fluid may be optimally increased by suspending three distinct kinds of nanoparticles in it. Trihybridnanofuids are the name given to such fuids. In order to employ ternary hybrid nanofluid flow, Sundar et al. [70] suspended GO, Fe3O4, and TiO2 nanoparticles in ethylene glycol. The thermal performance of the flow system has increased by 1% to 3% and 12.24%, 14.32%, according to the authors' experimental work, which also included new equations for the estimate of Nusselt number and thermophysical characteristics. Several authors of Sahoo [70], Manjunatha et al. [41], Shah et al, [61], Ahmed et al.,[1], Dezfulizadeh et al.[11]]

have inspected the irreversibility and thermal flow by usingdifferent shapes of nanoparticles in trihybrid nanofluid.

Nanofluid rotational flows have also attracted a lot of interest. Because of the nanofluid's rotation, these investigations use Coriolis body force words. Convective instability in a thin layer of a rotating magnetic nanofluid was examined by (Beg et al. [3]), taking into account thermophoresis, magnetophoresis, and Brownian diffusion. They discovered that, for magnetic nanofluids based on water and ester, the buoyancy mechanism is dominated by the magnetic field in fluid layers that are around 1 mm thick. This was determined by using a Chebyshev pseudo spectral numerical approach and taking into account various boundary conditions. Many authors (Hamad and Pop [18], Nadeem and Saleem [46], Rana et al. [52], Sheikholeslami et al. [64],) used both homotopy and Adomian decomposition methods, as well as the fourth-order Runge–Kutta method, to analyse a homotopy analysis method (HAM) of the transient stagnation-point boundary layer flow of nanofluids from a spinning sphere in a rotating parallel plate channel system, taking into account copper, silver, alumina, and titanium oxide nanoparticles suspended in

In many areas of natural science, such as engineering, geophysics, and astrophysics, nonlinear convection flow of fluid is essential. Ibrahim and Gamachu [28] have examined the nonlinear convective fluid flow across an aradial stretching surface while taking these significant applications into consideration. This investigation concludes that an increase in magnetic and thermophoresis components has increased the fluid's mass and thermal diffusivities. The effect of slip conditions for a nonlinear convective nanofluid flow across an astretched surface has been discussed by Shaw et al. [63]. After calculating the numerical solution for the governing partial differential equations, the authors came to the conclusion that the Sherwood and Nusselt numbers had increased with increasing convective factor values. Waqas et al. [79], Hong et al. [26], Hayat et al. [21] inspected MHD fluid flow with nonlinear convection over the convective heated surface with variable thickness.

Nonlinear mathematical form of thermal radiation isused in those cases whenever the more general form of theradiation phenomenon for a fluid flow problem is required.(ermal radiations have numerous applications in engi-neering and material sciences such as manufacturing ofglass, polymer fabrication, coolant of atomic reactors, andfurnace design. Moreover, thermal radiations also havefruitful applications in space modernization genetic factorssuch as rockets, rocket streamlines features, propulsionsystem, and operating system of space craft at the highertemperature. Due to its important applications, many investigations have been conducted ([Waqas et al [80], Sadeghi et al[56], Waqas [77], [Khan et al[33], Hayat et al[22], Shaw et al.[62], Rooman et al. [55]) with the mainfocus on the utilization of thermal radiations by employingthe linear form of Rosseland flow.

Because of its numerous applications in various technical and industrial domains, MHD has attracted the attention of scientists and researchers. Numerous technological and industrial processes, including chemical processing, drug targeting, power generation, air conditioners, petroleum production, MHD sensors, magnetic hyperthermia, MRI, magnetic therapy, and more, can benefit from the practical applications of magnetohydrodynamics. The effect of the chemical reaction on the three-dimensional flow of Maxwell nanofluid across a stretched surface with a magnetic field was investigated by Reddy and Lakshminarayana [54]. In their discussion of the MHD flow of a hybrid nanofluid including silver Ag and titanium oxide (TiO_2) nanoparticles towards an exponentially extending surface through a porous medium, Krishna et al. [35] discovered an increase in the magnetic parameter. Haider et al. [17] considered the influence of activation energy and thermal radiation on the dynamic flow of nanofluid over a stretching surface with magnetic field impact. With the use of the Runge-Kutta method, the simulation of the problem is performed. Some significant work on the MHD flow problems in various geometries can be cited in Refs. (Tassaddiq et al. [71], Waini et al. [74], Kalpana et al. [30], Arif et al. [2], Shoaib et al. [68] [Ramzan et al [49, 50, 51]).

Novelties of the present study

The study considers a $Cu–Al_2O_3–Ag$/ethylene-glycol ternary nanofluid, combining three different nanoparticles to investigate enhanced thermal and transport characteristics compared with conventional base fluids. A major novelty is the simultaneous consideration of MHD, mixed convection, squeezing, rotation, thermal radiation, non-uniform heat sources, and activation energy in a single mathematical model. This provides a more comprehensive representation of complex thermal-fluid systems. The incorporation of both channel rotation and squeezing motion provides an important extension of conventional nanofluid flow models and allows the influence of rotational and wall-motion effects on heat and mass transfer to be examined. The inclusion of activation energy accounts for the temperature-sensitive nature of chemical reactions. Its interaction with thermal radiation and internal heat generation provides a realistic framework for reactive thermal systems and considering irregular/spatially varying heat sources makes the model more physically realistic for engineering systems where heat is not generated uniformly throughout the fluid domain.

Real-Time Applications

1. $Cu–Al_2O_3–Ag$/ethylene-glycol nanofluids can be considered for compact and high-performance heat exchangers, where enhanced thermal transport and controlled fluid motion are desirable.
2. The rotating-channel configuration is relevant to rotating machinery, cooling of rotating components, rotating heat exchangers and thermal management systems where centrifugal and Coriolis effects influence fluid transport.
3. The simultaneous inclusion of activation energy, heat generation and thermal radiation makes the model applicable to exothermic chemical reactors and reactive processing equipment, where reaction rates and temperature control are important.
4. The model can contribute to the analysis and optimization of solar thermal systems, thermal energy storage, power-generation equipment and other energy-conversion technologies involving radiative heat transfer.

The main objective of the present investigation is to study MHD effects on the three dimensional squeezing flow of an electrically conducting in a rotating channel and its heat and mass transfer characteristics. To the best of author's knowledge, such study has not received attention in the engineering sciences literature so far. The governing equations are reduced to set of ordinary differential equations and then numerically solved by employing Runge-Kutta-Fehlberg fourth-fifth order method. Effect of pertinent parameters on velocity, temperature and nanoconcentration fields is examined through the plots. Skin-friction coefficients, Nusselt number and Sherwood number for different variations are studied numerically. The authors have hope that the results obtained in the present study not only provide useful information for applications, it also serves as a complement to the previous studies.

2. Mathematical Formulation

Consider an unsteady three-dimensional squeezing flow of an electrically conducting incompressible nanofluid in a vertical rotating channel. The plane positioned at $y = 0$ is a rest and maintained at the constant temperature T_0 and concentration Co. The temperature at the other plane is T_h and located at a variable distance $h(t)=\sqrt{\nu_f(1-\alpha t)}$. In negative *y*-direction, the fluid is squeezed with a time dependent velocity $V_h = dh/dt = -\alpha/2\sqrt{\nu_f/\alpha(1-\alpha t)}$. The fluid and the channel are rotated about *y*-axis with angular velocity $\vec{\Omega}=\omega\hat{j}/(1-\alpha t)$. The transverse magnetic field is assumed to be variable kind $\vec{B}=B_0/\sqrt{(1-\alpha t)}$ and it is applied along *y*-axis. The fluid is sucked/injected from the plane located at *y* = 0 as shown in figure 1. The magnetic Reynolds number is assumed to be small thus induced magnetic field is negligible. In addition, effects of Hall current, viscous dissipation and Joule heating are neglected.

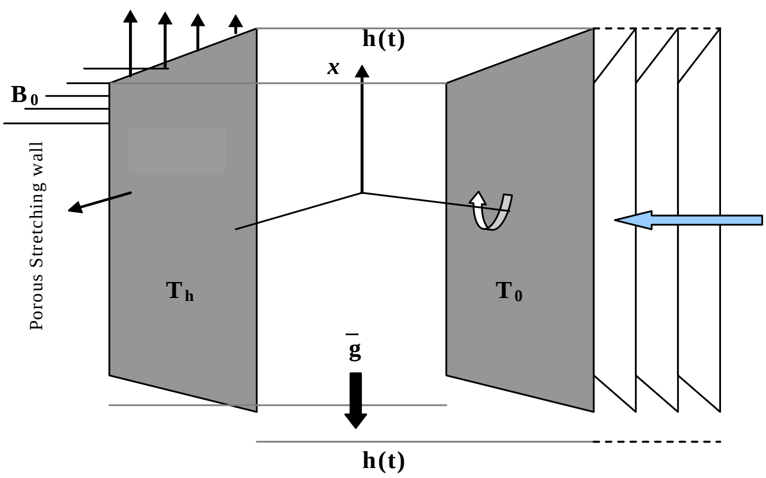

Fig. 1 Flow configuration and coordinate system

Under those assumptions, the governing equations for the velocity and temperature fields in the presence of internal heating source/sink are given by [*Hayat et al* 2015], *Munawar et al* 2012].

$$\frac{\partial u}{\partial x}+\frac{\partial v}{\partial y}=0, \tag{2.1}$$

$$\frac{\partial u}{\partial t}+u\frac{\partial u}{\partial x}+v\frac{\partial u}{\partial y}+2\frac{\omega}{1-\alpha t}w=-\frac{1}{\rho_{thnf}}\frac{\partial p}{\partial x}+\frac{\mu_{thnf}}{\rho_{thnf}}[(\frac{\partial^2 u}{\partial x^2}+\frac{\partial^2 u}{\partial y^2})]$$
$$-\frac{\sigma B_0^2}{\rho_{thnf}(1-\alpha t)}(u+mw)+\frac{g(\rho\beta_T)_{thnf}}{\rho_{nf}}(T-T_0)-(\frac{\mu_{thnf}}{k})u-\frac{C_B}{\sqrt{k}}\mathrm{u}^2, \tag{2.2}$$

$$\frac{\partial v}{\partial t}+u\frac{\partial v}{\partial x}+v\frac{\partial v}{\partial y}=-\frac{1}{\rho_{thnf}}\frac{\partial p}{\partial y}+\frac{\mu_{thnf}}{\rho_{thnf}}[\frac{\partial^2 v}{\partial x^2}+\frac{\partial^2 v}{\partial y^2})]-(\frac{\mu_{thnf}}{k})\mathrm{v}-\frac{C_B}{\sqrt{k}}\mathrm{v}^2, \tag{2.3}$$

$$\frac{\partial w}{\partial t}+u\frac{\partial w}{\partial x}+v\frac{\partial w}{\partial y}=\frac{\mu_{thnf}}{\rho_{thnf}}[\frac{\partial^2 w}{\partial x^2}+\frac{\partial^2 w}{\partial y^2})]+\frac{\sigma B_0^2}{\rho_{thnf}(1-\alpha t)}(mu-w)-(\frac{\mu_{thnf}}{k})\mathrm{w}-\frac{C_B}{\sqrt{k}}\mathrm{w}^2, \tag{2.4}$$

$$\frac{\partial T}{\partial t}+u\frac{\partial T}{\partial x}+v\frac{\partial T}{\partial y}=\frac{k_{thnf}}{(\rho C_p)_{thnf}}\left(\frac{\partial^2 T}{\partial x^2}+\frac{\partial^2 T}{\partial y^2}\right)+\frac{1}{(\rho C_p)_{thnf}(1-\alpha t)}[q'''-\frac{\partial(q_R)}{\partial y}+Q_1^{'}(C-C_0)]+$$
$$+\frac{2\mu_{thnf}}{(\rho C_p)_{thnf}}[(\frac{\partial u}{\partial y})^2+(\frac{\partial v}{\partial y})^2]+\frac{\sigma_{thnf}\mu_e^2 H_o^2}{(\rho C_p)_{thnf}}(u^2+v^2) \tag{2.5}$$

$$\frac{\partial C}{\partial t}+u\frac{\partial C}{\partial x}+v\frac{\partial C}{\partial y}=D_m\left(\frac{\partial^2 C}{\partial x^2}+\frac{\partial^2 C}{\partial y^2}\right)-\frac{k_c}{(1-\alpha t)}(C-C_0)(\frac{T}{T_o})^n Exp(-\frac{E_a}{KT})+ +\frac{D_m K_T}{T_m}\left(\frac{\partial^2 T}{\partial x^2}+\frac{\partial^2 T}{\partial y^2}\right), \quad (2.6)$$

where u, v and w are velocity components along x,y and z directions respectively, p is pressure. B_0 is the magnetic field, σ is the electrical conductivity, g is the magnitude of acceleration due to gravity, α is characteristic parameter with the dimension of reciprocal of time t and $\alpha t < 1$. T is temperature of the fluid .

The coefficient q''' is the rate of internal heat generation (>0) or absorption(<0). The internal heat generation /absorption q''' is modelled as

$$q'''=(\frac{k_f}{a^2 v})(A_{11}^{'}(T_w-T_0)u+B_{11}^{'}(T-T_0)) \quad (2.5)$$

where $A_{11}^{'}$ and $B_{11}^{'}$ are coefficients of space dependent and temperature dependent internal heat generation or absorption respectively. It is noted that the case $A_{11}^{'}$>0 and $B_{11}^{'}$>0, corresponds to internal heat generation and that $A_{11}^{'}$<0 and $B_{11}^{'}$<0, the case corresponds to internal heat absorption case.

Thermo Physical Properties

The properties associated with the thermal and physical behaviour of nanoparticles when joined with Ethylene Glycol as the primary medium can be disclosed in Table.1

The characteristics of standard and innovative nanofluids ,encompassing density. heat capacity, thermal expansion rate, electrical and thermal conductivities as well as viscosity, are outlined in subsequent manner

Viscosity: $$\mu_{nf}=\frac{\mu_f}{(1-\phi_1)^{2.5}}\ ,\mu_{hnf}=\frac{\mu_f}{(1-\phi_1-\phi_2+\phi_1\phi_2)^{2.5}},\mu_{thnf}=\frac{\mu_f}{[(1-\phi_1)(1-\phi_2)(1-\phi_3)]^{2.5}}$$

Density:

$$\rho_{nf}=\rho_f[(1-\phi_1)+\phi_1\rho_{s1}]\ ,\rho_{hnf}=\rho_f[(1-\phi_1)(1-\phi_{s_1})+\phi_1(1-\phi_2)\rho_{s1}]+\phi_1\phi_2\rho_{s2}],$$

$$\rho_{thnf}=\rho_f[(1-\phi_1)(1-\phi_{s_1}+\frac{\rho_{s1}}{\rho_f}\phi_1)+\frac{\rho_{s2}}{\rho_f}\phi_2]+\frac{\rho_{s3}}{\rho_f}\phi_3$$

Heat capacity:

$$(\rho C_p)_{nf}=(\rho C_p)_f[(1-\phi_1)+\phi_1\rho_{s1}]\ ,(\rho C_p)_{hnf}=(\rho C_p)_f[(1-\phi_1)(1-\phi_{s_1})+\phi_1(1-\phi_2)(\rho C_p)_{s1}]+\phi_2(\rho C_p)_{s2}],$$

$$(\rho C_p)_{thnf}=(\rho C_p)_f(1-\phi_3)[(1-\phi_2)(1-\phi_1+\frac{(\rho C_p)_{s1}}{(\rho C_p)_f}\phi_1)+\frac{(\rho C_p)_{s2}}{(\rho C_p)_f}\phi_2]+\frac{(\rho C_p)_{s3}}{(\rho C_p)_f}\phi_3$$

Thermal Expansion factor:

$$\beta_{nf}=\beta_f[(1-\phi_1)+\phi_1\beta_{s1}]\ ,\beta_{hnf}=\beta_f[(1-\phi_1)(1-\phi_{s_1})+\phi_1(1-\phi_2)\beta_{s1}]+\phi_1\phi_2\beta_{s2}],$$

$$\beta_{thnf}=\beta_f[(1-\phi_1)(1-\phi_{s_1}+\frac{\beta_{s1}}{\beta_f}\phi_1)+\frac{\beta_{s2}}{\beta_f}\phi_2]+\frac{\beta_{s3}}{\beta_f}\phi_3$$

Thermal conductivity:

$$\frac{k_{nf}}{k_f}=\frac{k_{s1}+2k_f-2\phi_1(k_f-k_{s1})}{k_{s1}+2k_f+\phi_1(k_f-k_{s1})},\frac{k_{hnf}}{k_{nf}}=\frac{k_{s2}+2k_{nf}-2\phi_2(k_{nf}-k_{s2})}{k_{s2}+2k_{nf}+\phi_2(k_{nf}-k_{s2})},$$

$$\frac{k_{thnf}}{k_{hnf}}=\frac{k_{s3}+2k_{hnf}-2\phi_3(k_{hnf}-k_{s3})}{k_{s3}+2k_{hnf}+\phi_3(k_{hnf}-k_{s3})}$$

Electrical conductivity:

$$\frac{\sigma_{nf}}{\sigma_f}=\frac{\sigma_{s1}+2\sigma_f-2\phi_1(\sigma_f-\sigma_{s1})}{\sigma_{s1}+2\sigma_f+\phi_1(\sigma_f-\varpi_{s1})},\frac{\sigma_{hnf}}{\sigma_{nf}}=\frac{\sigma_{s2}+2\sigma_{nf}-2\phi_2(\sigma_{nf}-\sigma_{s2})}{\sigma_{s2}+2\sigma_{nf}+\phi_2(\sigma_{nf}-\sigma_{s2})},$$

$$\frac{\sigma_{thnf}}{\sigma_{hnf}}=\frac{\sigma_{s3}+2\sigma_{hnf}-2\phi_3(\sigma_{hnf}-\sigma_{s3})}{\sigma_{s3}+2\sigma_{hnf}+\phi_3(\sigma_{hnf}-\sigma_{s3})} \tag{2.6}$$

hence ϕ is the solid volume friction of the nanofluid, ρ_f is the density of base fluid, ρ_s is the density of the nanoparticle. μ_f is the dynamic viscosity of the base fluid, $(\rho C_p)_f$ is the heat capacity of the base fluid, $(\rho C_p)_s$ is the heat capacity of the nanoparticle, k_f is the thermal conductivity of the base fluid and k_s is the thermal conductivity of nanoparticles.

Table.1 Physical properties of nanoparticles

Physical properties	**Fluid phase (Ethylene Glyc0l)**	**Copper**	**Al_2o_3 (Alluminium Oxide)**	**Ag (Silver)**
Cp(j/kg K)	2430	385	765	235
ρ(kg m3)	1115	8933	3970	10500
k(W/m K)	0.253	401	40	401
βx10-5 1/k)	5.7	1.67	0.85	1.89
ϕ	0.05	0.0	0.05	0.2
σ (S/m)	10.7×10^{-5}	5.96×10^{-7}	1.0×10^{-10}	6.3×10^{-6}

The approximate boundary conditions for the present problem are;

$$u(x,y,t)=0,\quad v(x,y,t)=0,\quad w(x,y,t)=0,\quad T(x,y,t)=T_0, C(x,y,t)=C_0 \qquad \text{at } y=0 \tag{2.7}$$

$$u(x,y,t)=0,\quad v(x,y,t)=V_h,\quad w(x,y,t)=0,\quad T(x,y,t)=T_h, C(x,y,t)=C_h \qquad \text{at } y=h(t) \tag{2.8}$$

where $T_h=T_0+T_0/(1-\alpha t), C_h=C_0+C_0/(1-\alpha t), V_{w0}=-V_0/(1-\alpha t)$. Here V_0 is constant, $V_{w0}<0$ corresponds injection whereas $V_{w0}>0$ corresponds wall suction.

To reduce the governing equations into a set of similarity equations, introduce the following similarity transformations [*Munawar et al* 2012].

$$\psi = \sqrt{\frac{\alpha v_f}{1-\alpha t}}\, x f(\eta),\ \eta = \frac{y}{h(t)}, T = T_0 + \frac{T_0}{1-\varepsilon t}\theta(\eta), \Phi = C_0 + \frac{C_0}{1-\varepsilon t}C(\eta),$$

$$u = U_{w0} f_\eta \eta, \qquad v = -\sqrt{\frac{\alpha v_f}{1-\alpha t}}\, f(\eta), \qquad w = U_{w0} g(\eta), \qquad (2.9)$$

where a suffix η denote the differentiation with respect to η and v_f is the kinematic viscosity of the base fluid. Using the above transformations (2.9), the equation (2.1) is automatically satisfied, while the equation (2.2) – (2.5) are respectively reduces to the following nonlinear ordinary differential equations;

$$f_{\eta\eta\eta} = \left[f\, f_{\eta\eta} - f_\eta^2 - \beta\left(f_\eta \frac{\eta}{2} f_{\eta\eta}\right) + 2Rg - A_2 A_6 (M^2 + D^{=1}) f_\eta - fs(f_\eta)^2 + A_4 Gr\theta \right] = \frac{(1-\alpha t)^2}{a^2 x}\frac{\partial p}{\partial x}, \qquad (2.10)$$

$$f_{\eta\eta} + \left[-f\, f_\eta + \frac{\beta}{2}\left(f + \eta f_\eta \right)\right] - D^{-1} f - fs(f^2) = -\frac{(1-\alpha t)}{\mu_{thnf}\, a} p_\eta, \qquad (2.11)$$

$$g_{\eta\eta} + (\left[f\, g_\eta - f_\eta g - \beta\left(g \frac{\eta}{2} g_\eta \right)\right] - 2Rf_\eta - A_2 A_6 (M^2 + D^{-1}) g) - \mathrm{fs}(g^2) = 0, \qquad (2.12)$$

$$(A_5 + \frac{4Rd}{3})\theta_{\eta\eta} + \Pr\left[A_4 \left\{ \beta\left(\theta + \frac{\eta}{2}\theta_\eta\right) + f\theta_\eta \right\} + A_{11} f' + B_{11}\theta \right]$$
$$+ A_5[2Ec\Pr\{(\frac{\partial^2 f}{\partial \eta})^2 + (\frac{\partial g}{\partial \eta})^2\} + \mathrm{M}^2 \mathrm{Ec}\Pr A_6\{(\mathrm{f}')^2 + g^2\}] = 0 \qquad (2.13)$$

$$\Phi_{\eta\eta} - Sc\left(\left\{ \beta\left(\Phi + \frac{\eta}{2} C_\eta \right) + f\Phi_\eta \right\} - \gamma\,\varepsilon(1 + n\delta\theta) Exp(-\frac{E_1}{1+\delta\theta}) + Sr\,\theta_{\eta\eta} \right) = 0$$

Reduced boundary conditions are;

$f_\eta = 0,\ f = 0,\quad g = 0,\quad \theta = 0\ ,\ \Phi=0 \qquad$ at $\qquad \eta = 0$

$f_\eta = 0,\ f = \frac{\beta}{2},\quad g = 0,\quad \theta = 1\ ,\ \Phi=1 \qquad$ at $\qquad \eta = 1 \qquad$ (2.14)

where

$\beta = \alpha/a$ is the squeezing parameter, $m = \omega_e \tau_e$ is Hall parameter,

$M^2 = \sigma B_0^2 / \alpha\rho_f$ is magnetic parameter, $\mathrm{D}^{-1}(K) = \frac{L^2}{k}$ is the inverse Darcy parameter

$\mathrm{fs} = (\frac{C_B}{\sqrt{k}})$ is the Forchheimer parameter, $G = g\beta_f T_0 x^3 / v_f^2 (1-\alpha t)$ is modified Grashof number, $R = \omega / \alpha$ is rotation parameter, $Pr = (\mu c_p)_f / k_f$ is the Prandtl number, $A_{11} = \frac{A_{11}^{'}(1-\alpha t)}{a(\rho C_p)\mathrm{A}_4}$ (Space dependent heat source parameter), $B_{11} = \frac{B_{11}^{'}(1-\alpha t)}{a(\rho C_p)\mathrm{A}_4}$ (Temperature dependent heat source parameter), $Sc = \frac{v_f}{D_m}$ is the

Schmidt number, $E1=\dfrac{E_a}{KT_0}$, is the Activation energy parameter, $\theta_w=\dfrac{T_h}{T_o},\delta=\theta_w-1,$ is the temperature difference parameter, $Sr=\dfrac{D_m K_T T_0}{aT_m\ C_0}$ is the Soret parameter, $\gamma=\dfrac{kc}{a}$ *is the chemical reaction parameter*

$$A_1=(1-\phi_1)(1-\phi_2)(1-\phi_3)]^{2.5},\ A_2=[(1-\phi_1)(1-\phi_{s_1}+\frac{\rho_{s1}}{\rho_f}\phi_1)+\frac{\rho_{s2}}{\rho_f}\phi_2]+\frac{\rho_{s3}}{\rho_f}\phi_3$$

$$A_3=[(1-\phi_1)(1-\phi_{s_1}+\frac{\beta_{s1}}{\beta_f}\phi_1)+\frac{\beta_{s2}}{\beta_f}\phi_2]+\frac{\beta_{s3}}{\beta_f}\phi_3$$

$$A_4=(1-\phi_3)[(1-\phi_2)(1-\phi_1+\frac{(\rho C_p)_{s1}}{(\rho C_p)_f}\phi_1)+\frac{(\rho C_p)_{s2}}{(\rho C_p)_f}\phi_2]+\frac{(\rho C_p)_{s3}}{(\rho C_p)_f}\phi_3$$

$$A_5=\frac{k_{s3}+2k_{hnf}-2\phi_3(k_{hnf}-k_{s3})}{k_{s3}+2k_{hnf}+\phi_3(k_{hnf}-k_{s3})},\ A_6=\frac{\sigma_{s3}+2\sigma_{hnf}-2\phi_3(\sigma_{hnf}-\sigma_{s3})}{\sigma_{s3}+2\sigma_{hnf}+\phi_3(\sigma_{hnf}-\sigma_{s3})}$$

It is important to mention that, β = 0 represents plates are stationary, β > 0 corresponds to the plate which is located at $y = h(t)$ moves towards the plate which is located at $y = 0$ and β <0 corresponds to the plate at $y = y(t)$ moves apart with respect to the plate at $y= 0$.

Therefore expression for the local skin-friction coefficient and the local Nusselt number at both the walls are defined as;

$$C^*_{f,\ \text{at}\ y=0}=\frac{(\tau_{xy})_{y=0}}{\rho_{nf}U_{w0}^2},\qquad C^*_{f,\ \text{at}\ y=h(t)}=\frac{(\tau_{xy})_{y=h(t)}}{\rho_{nf}U_{w0}^2},\qquad (2.15)$$

$$Nu^*_{\ \text{at}\ y=0}=\sqrt{\frac{v_f}{a}}\frac{(q_{xy})_{y=0}}{k_f T_0},\qquad Nu^*_{\ \text{at}\ y=h(t)}=\sqrt{\frac{v_f}{a}}\frac{(q_{xy})_{y=h(t)}}{k_f T_0},\qquad (2.16)$$

where τ_{xy} is the shear stress and q_{xy} is the heat flux, which are given by

$$\tau_{xt}=\mu_{nf}\left(\frac{\partial u}{\partial x}+\frac{\partial u}{\partial y}\right)\ \text{and}\ \ q_{xt}=-k_{nf}\left(\frac{\partial T}{\partial x}+\frac{\partial T}{\partial y}\right)\qquad (2.17)$$

In view of equation (2.17) and similarity transformations (2.9); equations (2.15)-(2.17) will takes the following form;

$$C^*_{f,\ \text{at}\ y=0}=\sqrt{\text{Re}}\,C^*_{f,\ \text{at}\ y=0}=f_{\eta\eta}(0)/(1-\phi)^{2,5}\left(1-\phi+\phi\left(\frac{\rho_s}{\rho_f}\right)\right),$$

$$C^*_{f,\ \text{at}\ y=h(t)}=\sqrt{\text{Re}}\,C^*_{f,\ \text{at}\ y=h(t)}=f_{\eta\eta}(1)/(1-\phi)^{2,5}\left(1-\phi+\phi\left(\frac{\rho_s}{\rho_f}\right)\right),$$

$$Nu_{\ \text{at}\ y=0}=(1-\alpha t)^{1,5}\ Nu^*_{\ \text{at}\ y=0}=-\frac{k_{nf}}{k_f}\theta_\eta(0),$$

$$Nu_{\ \text{at}\ y=h(t)}=(1-\alpha t)^{1,5}\ Nu^*_{\ \text{at}\ y=h(t)}=-\frac{k_{nf}}{k_f}\theta_\eta(1)$$

$$Sh_{\ \text{at}\ y=0}=(1-\alpha t)^{1,5}\ Sh^*_{\ \text{at}\ y=0}=-C_\eta(0),$$

$$Sh_{\ \text{at}\ y=h(t)}=(1-\alpha t)^{1,5}\ Sh^*_{\ \text{at}\ y=h(t)}=-C_\eta(1)\qquad (2.18)$$

3. Comparison

In the absence of mass concentration, thermal radiation (Rd=0), Soret effect (Sr=0), chemical reaction (γ=0) the results are in good agreement with those of Mahantesh et al [2016]

Parameters					Mahantesh et al [2016]				**Present results**			
M	R	β	Q	ϕ	$\tau_x(0)$	$\tau_x(1)$	Nu(0)	Nu(1)	**$\tau_x(0)$**	**$\tau_x(1)$**	**Nu(0)**	**Nu(1)**
0.5	1	1	1	0.1	-7.0265	3.3384	-1.5293	-2.7822	**-7.0263**	**3.3381**	**-1.5296**	**-2.7820**
2					-7.1046	3.4001	-1.5294	-2.7828	**-7.1042**	**3.3999**	**-1.5299**	**-2.7829**
4					-7.2073	3.4804	-1.5281	-2.7934	**-7.2069**	**3.4811**	**-1.5280**	**-2.7936**
	2				-5.5791	2.4747	-1.5202	-2.7853	**-5.5783**	**2.4739**	**-1.5204**	**-2.7852**
	4				-0.1112	0.0093	-1.4743	-2.8187	**-0.1111**	**0.0092**	**-1.4748**	**-2.8184**
		2			-5.5659	2.5073	-1.3298	-4.2217	**-5.5649**	**2.5069**	**-1.3299**	**-4.2212**
		3			-4.0516	1.5507	-1.0860	-5.2527	**-4.0512**	**1.5507**	**-1.0862**	**-5.2522**
			2		-5.8765	2.0045	-1.7484	-2.2084	**-5.8759**	**2.0045**	**-1.7488**	**-2.2079**
			4		-4.9876	1.9876	-1.88976	-2.0076	**-4.9869**	**1.9871**	**-1.8897**	**-2.0076**
				0.15	-8.2534	3.9573	-1.2162	-2.7076	**-8.2534**	**3.9576**	**-1.21659**	**-2.7071**
				0.20	-7.0458	3.3369	-1.6181	-3.2448	**-7.0458**	**3.3373**	**-1.6179**	**-3.2443**

4. Numerical Method and Validation

A set of non-similar equations (2.15)-(2.17) are nonlinear in nature and possess no analytical solution, thus, a numerical treatment would be more appropriate. These set of ordinary differential equations together with the boundary conditions (2.14) are numerically solved by employing fourth-fifth order Runge-Kutta-Fehlberg scheme with the help of Maple. This algorithm in Maple is proven to be precise and accurate and which has been successfully used to solve a wide range of nonlinear problem in transport phenomena especially for flow and heat transfer problems. In this study, we set the relative error tolerance to 10^{-6}. Comparison results are recorded in table 1 and are found to be in excellent agreement. The effects of development of the squeezing three-dimensional flow and heat transfer in a rotating channel utilizing nanofluid are studied for different values of squeezing parameter, rotation parameter, magnetic parameter, suction/injection parameter, mixed convection parameter, nanoparticle volume fraction parameter, Prandtl number, radiation parameter, Schmidt number, Soret parameter, Chemical reaction parameter and heat source/sink parameter. In the following section, the results are discussed in detail with the aid of plotted graphs and tables.

5. Discussion of the Numerical Results

We make an investigation of the three dimensional non-Darcy squeezing hydromagnetic convective flow ,heat and mass transfer flow of an electrically conducting Ethylene Glycol based Cu+Al2O3+Ag/Eg ternary/hybrid nanofluid in a vertical channel in the presence of irregular heat source. In our numerical simulation the default values of the parameters are considered as: M^2=0.5,, A11=0.5,B11=0.5,.R=0.5,m=0.5, β=0.5, Pr=0.71, Sc=1.3, Sr=05, γ=0.5, Rd=0.5, Q1=0.5,E1=0.1,δ=0.2,n-=0.2. In order to analyze the effects of various pertinent parameters on velocity, temperature and nanoconcentration profiles, several graphs are plotted. In all parametric variations, we follow the convention that the non-dimensional temperature and nanoconcentration are positive/negative according as the actual temperature (θ) / Concentration (Φ) are greater/lesser than the ambient temperature (To) /Concentration(Co).

The numerical results demonstrate that the ternary/hybrid Cu–Al_2O_3–Ag/ethylene-glycol nanofluid exhibit distinct responses to the governing physical parameters. The effects are presented in terms of axial velocity f', secondary velocity g, temperature θ, and nanoparticle concentration Φ.

The effect of nanoparticle volume fraction (ϕ) on f', g, θ and Φ can be seen from the figs.2a-2d. As the volume fraction increases, the thermal conductivity of the nanofluid is elevated. Therefore thermal diffusion is associated in the regime. It can be found from the profiles that an increase in nanoparticle volume fraction leads to a depreciation in the region (0,1.0) while the secondary velocity(g) grows in the entire flow region in both ternary and hybrid nanofluids. This may be attributed to the fact that the thickness of the momentum boundary layer reduces with increase in ϕ. Also the thickness of the thermal boundary layer becomes thicker and solutal boundary layer becomes thinner with increase in ϕ which leads to a rise in temperature and fall in nano concentration in the flow region in Ethylene Glycol based ternary and hybrid(figs.2c&2d).

Figure.3 are plotted for f',g,θ and Φ profiles against η for different values of G by fixing other parameters. Analysis of the Fig. 3, Increasing Grashof number (G)from 2 to 6 significantly modifies both velocity components. Physically, a larger Grashof number represents stronger thermal buoyancy relative to viscous forces, which enhances the buoyancy-driven motion of the fluid. The resulting changes in θ and Φ indicate that stronger convection also influences thermal and nanoparticle transport.

For M=0.5,1.0,1.5,(Fig.4) the velocity profiles change considerably. Physically, increasing M strengthens the Lorentz force(Magnetic parameter(M)), which acts as an electromagnetic resistance to the fluid motion. This suppresses/controls momentum transport and consequently modifies the temperature and concentration distributions. Thus, an applied magnetic field provides an effective mechanism for controlling the flow.

An increase in Squeezing parameter (β) from 0.2 to 0.6 represents stronger squeezing of the fluid region. The compression modifies the velocity field and reduces the effective space available for fluid motion. Consequently, the thermal and concentration boundary layers are also altered. This demonstrates the importance of wall motion in controlling heat and mass transfer(Fig.5).

Increasing Forchheimer parameter (fs) from 0.1 to 0.3 introduces stronger inertial resistance in the porous medium. The fluid motion is therefore restricted, producing changes in both axial and secondary velocities. Since convection is modified, the temperature and nanoparticle concentration fields are also affected (Fig.6).

The profiles are examined for Rd=0.5,1.5,5.0. Increasing Thermal radiation parameter (Rd) strengthens radiative energy transport and significantly modifies the temperature distribution. Since temperature is coupled with momentum and concentration, corresponding changes occur in velocity and nanoparticle concentration. This effect is particularly important for high-temperature thermal systems(Fig.7).

Increasing Eckert number (Ec) from 0.1 to 0.3(Fig.8) represents stronger viscous dissipation, whereby mechanical energy is converted into thermal energy. Consequently, the temperature field is modified, which subsequently affects velocity and concentration. The effect becomes important when viscous heating cannot be neglected.

Figs.9a-9d and 10a-10d are plotted to illustrate the effect of space /temperature dependent heat source parameters (A11,B11) on the flow variables. It can be seen from the profiles that the axial velocity(f')and secondary velocity(g) augment with rising values of space /temperature dependent heat source parameters(A11.B11).This amount to the fact that the thickness of the momentum boundary layer becomes thicker with increase in A11/B11(figs.9a,9b,10a,10b).The thickness of the thermal boundary layer grows with larger values of space /temperature dependent heat sources((9c,10c).The nanoconcentration (Φ) reduces in Eg based ternary nanofluid while in Eg based ternary nanofluid it grows with increase in A11/B11.This may be attributed to the fact that in the presence of heat generating source, energy is generated in the flow region.(figs.9c&10c). The presence of heat generating / source, energy is generated in the flow region, which results in an enhancement in the temperature in both types of nanofluids.

The effect of Prandtl number(Pr) on f ′,g,θ and Φ can be seen from figs.11a-11d. Prndtl number refers to the relative contribution of momentum diffusion to thermal diffusion in the boundary layer regime. For Pr=0.71,1.71,6.20, increasing Pr corresponds to decreasing thermal diffusivity relative to momentum diffusivity. Therefore, thermal energy penetrates less deeply into the fluid and the thermal boundary layer becomes thinner. The calculated Nusselt number also decreases from approximately 0.1046 to 0.0758 for the ternary nanofluid as Pr increases, indicating a substantial change in wall heat-transfer characteristics.

The effect of Schmidt number (Sc) on f',g,θ and Φ is exhibited in fig.12a-12b. Increasing Schmidt number (Sc) from 0.24 to 1.30 represents lower mass diffusivity. Hence, the concentration boundary layer becomes thinner and the concentration gradient near the wall becomes stronger. This results in increasing species diffusion rates and lowering of nano-particle concentration magnitudes throughout the boundary layer. Physically this also manifests in a decrease in the nano-particle concentration boundary layer thickness with increasing Schmidt number. Also the momentum boundary layer thickness becomes thinner with increase in Schmidt number (Sc). The table confirms a strong increase in Sherwood number, from about 0.948 to 3.805 for the ternary nanofluid. Thus, Sc is an important parameter for controlling mass transfer.

The effect of thermo-diffusion on Φ is depicted in figs.13a-13b. Soret parameter Sr arises in the term, $+Sr(d^2\theta/d\eta^2)$ in the nanoconcentration conservation equation(2.18).This term represents the influence of temperature gradient on the concentration field. Increasing Soret parameter (Sr) from 0.25 to 1.0 enhances thermodiffusion, meaning that temperature gradients contribute more strongly to mass transport. The Sherwood number decreases from approximately 0.947 to 0.834 for the ternary nanofluid. Physically, stronger thermally induced diffusion redistributes species within the fluid and modifies the concentration gradient at the wall.

For γ=0.5,1.0,1.5, increasing the Chemical reaction parameter (γ)(Fig.14a-b) strength significantly affects the concentration field. This amounts to the fact that the thickness of the thermal and solutal boundary layers grow with γ>0 in both types of ternary and hybrid nanofluids Physically, stronger chemical reaction increases the rate of consumption or generation of the reactive species, thereby modifying concentration gradients and mass transfer. The Sherwood number increases from approximately 0.947 to 1.045 for the ternary nanofluid.

Figs.15a-15d represents temperature(θ) and nanoconcentration(Φ) with activation energy (E1). From the profiles that temperature and nanoconcentration experience enhancement with rising values of activation energy parameter(E1).This is due to the fact that increase in E1 leads to rise in the thickness of the thermal and solutal boundary layers which results in a augmentation in θ and Φ in the boundary layers. From figs.21a&21b it is observed that the thickness of the momentum boundary layer flows with larger values of activation energy(E1). The corresponding Sherwood number increases from approximately 0.947 to 1.045, indicating that activation energy has a measurable influence on mass transport. Physically, activation energy determines the sensitivity of the chemical reaction to the local thermal environment.

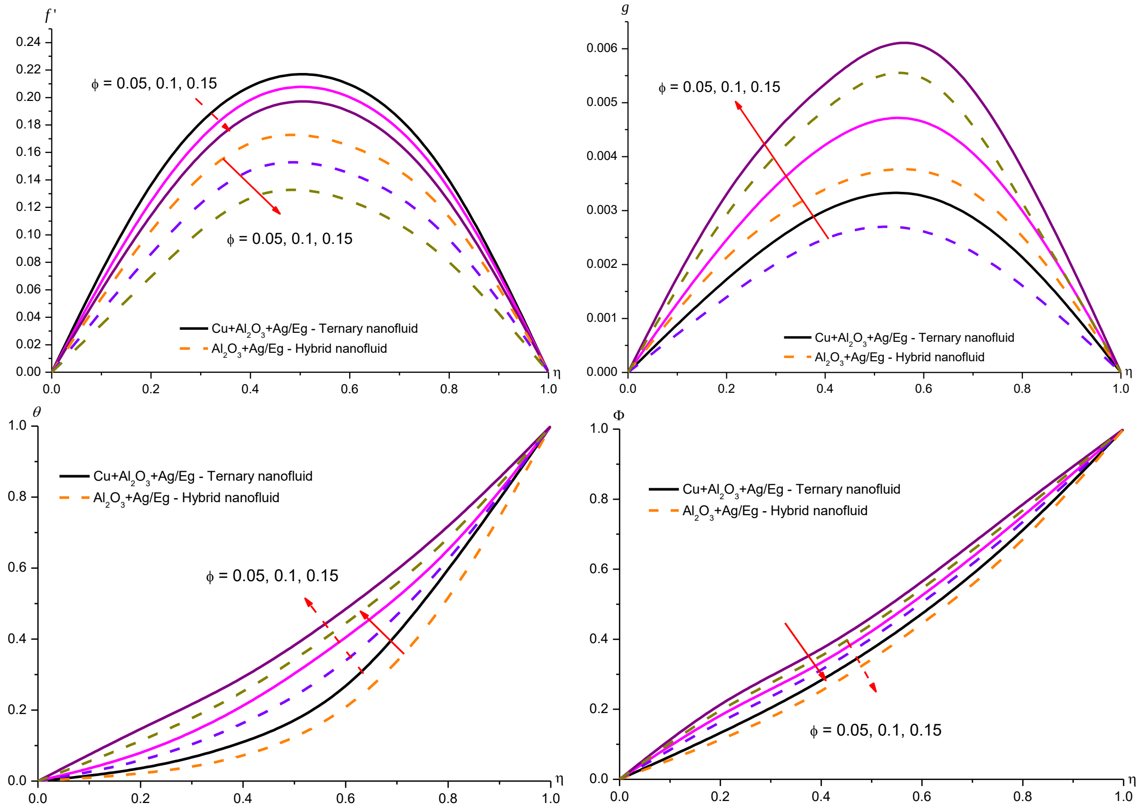

Fig.2 : Variation with $Cu+Al_2O_3+Ag/Eg$ ternary/hybrid of [a] axial velocity(u), [b] Secondary velocity(g), [c] Temperature(θ), [d] Nano-Concentration (Φ) with ϕ

G=2, M=0.5, fs=0.1, β=0.2, Rd=0.5, Ec=0.1, A11=0.5, B11=0.5, Pr=0.71, Sc=0.24, Sr=0.25, γ=0.5, E1=0.2

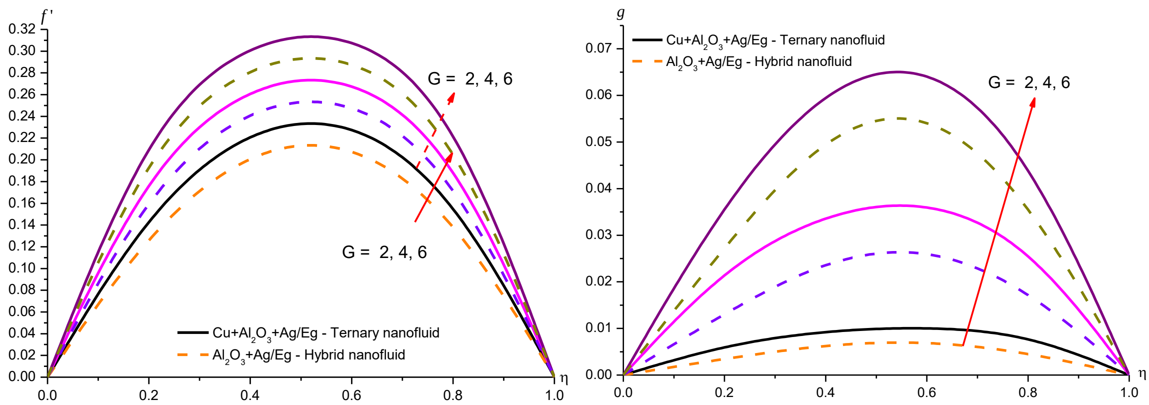

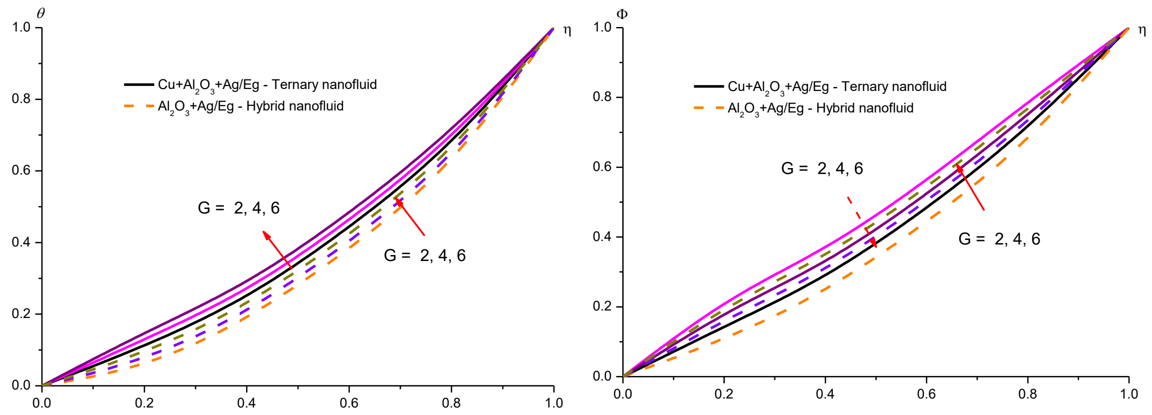

Fig.3 : Impact of G(Grashof number) on f', g, θ,Φ

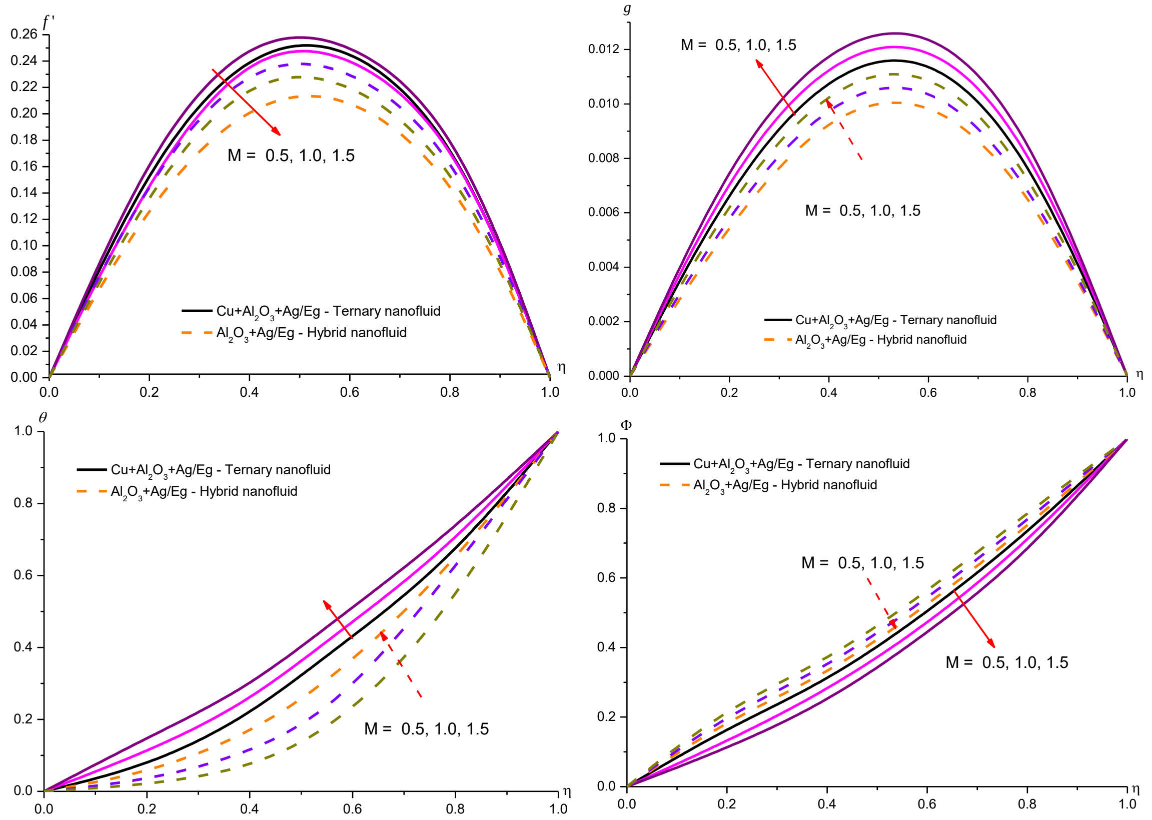

Fig.4 : Impact of M(Magnetic parameter) on f', g, θ,Φ

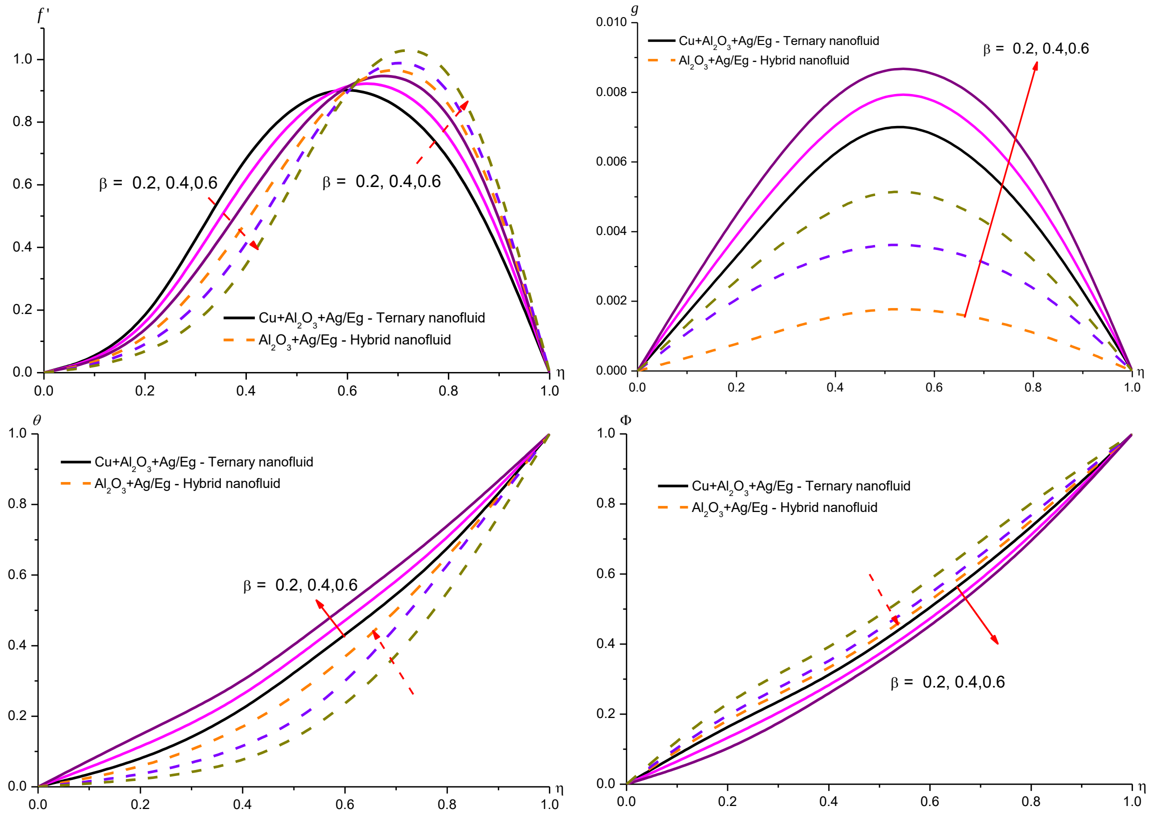

Fig.5 : Impact of β(squeezing parameter) on *f '*, *g*, θ,Φ

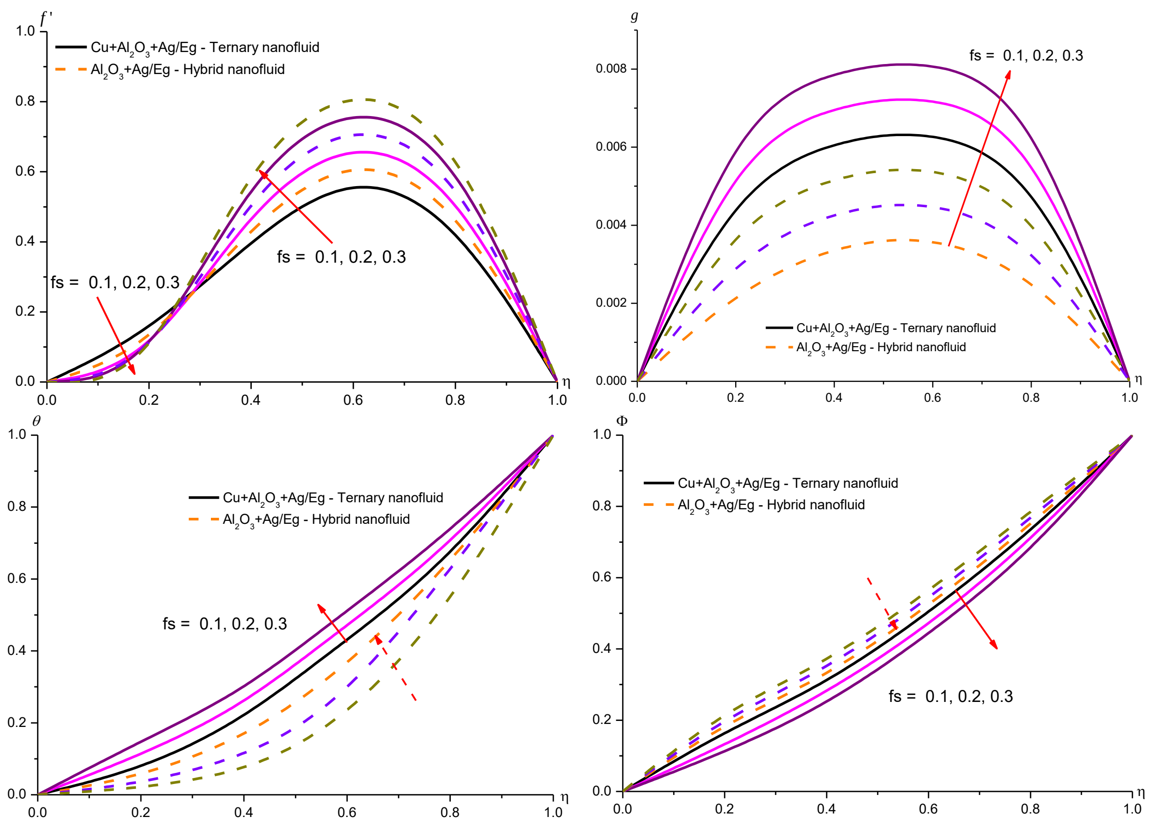

Fig.6 : Impact of fs(Forchheimer parameter) on *f '*, *g*, θ,Φ

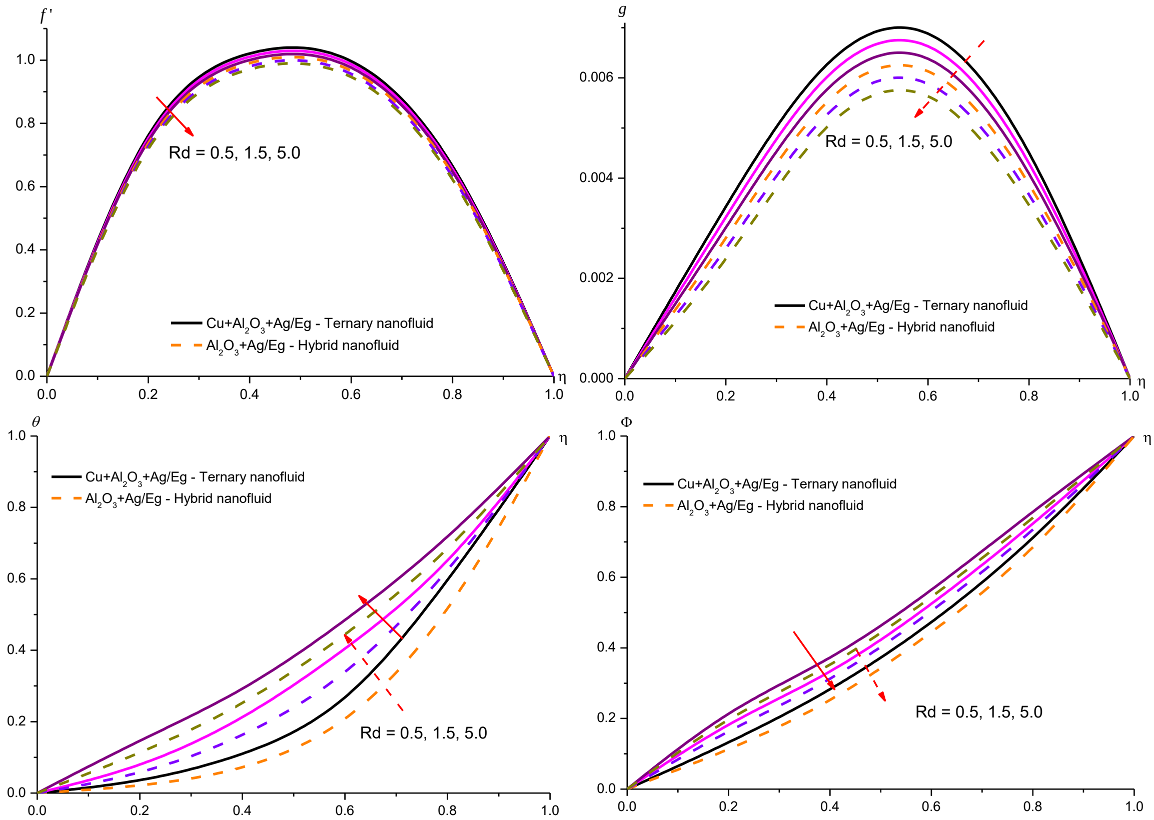

Fig.10 : Impact of Rd(Thermal Radiation) on f', g, θ, Φ

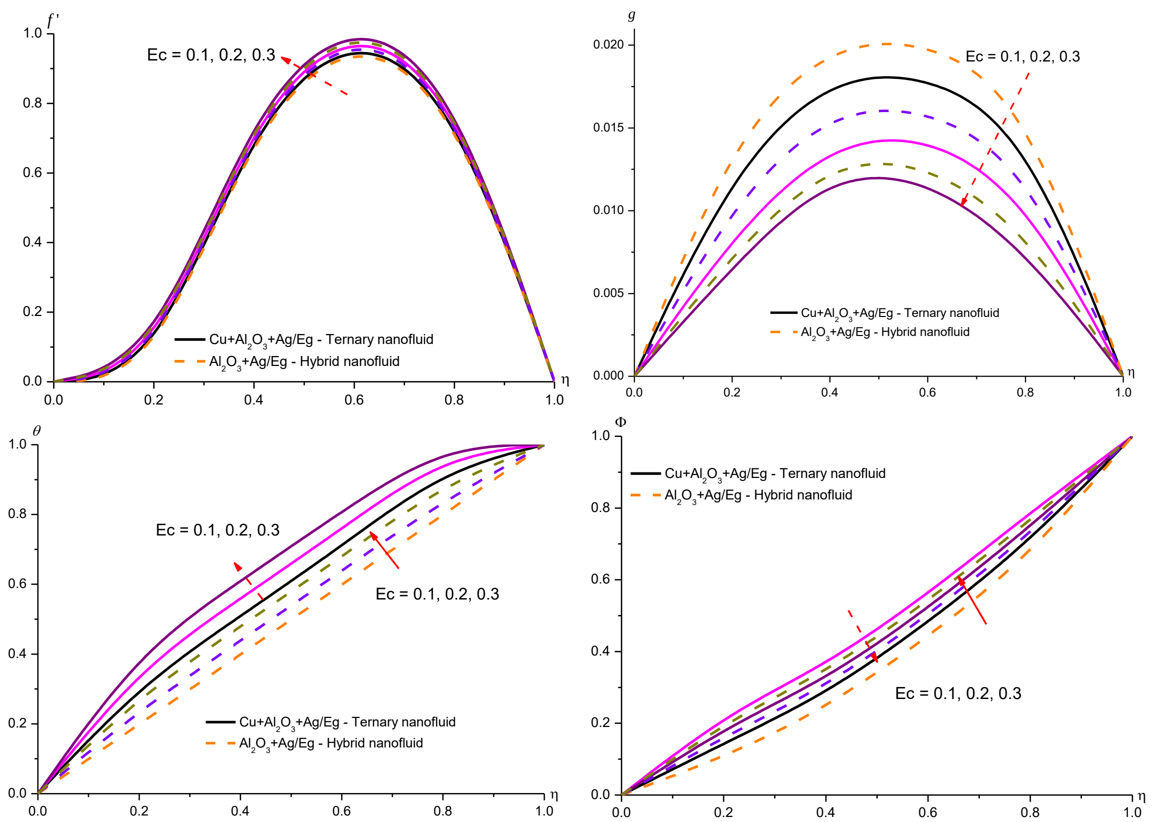

Fig.11 : Impact of Ec(Eckert number) on f', g, θ, Φ

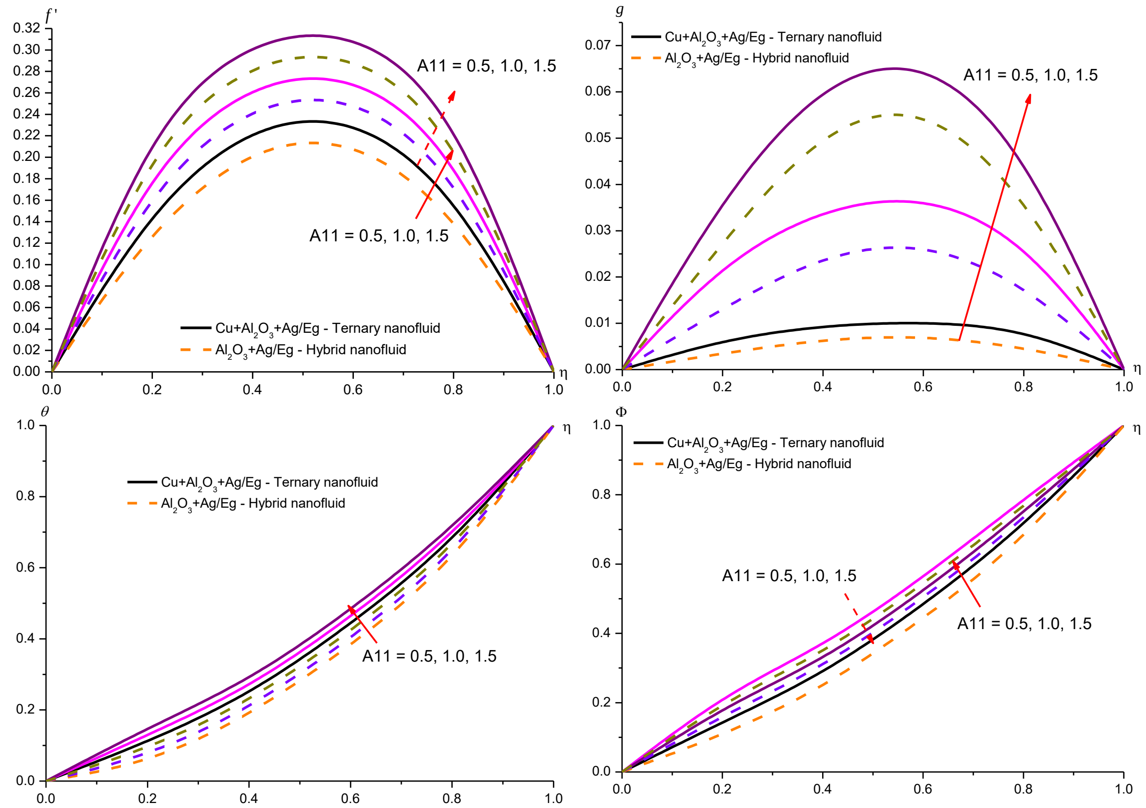

Fig.12 : Impact of A11(space dependent heat source parameter) on f', g, θ,Φ

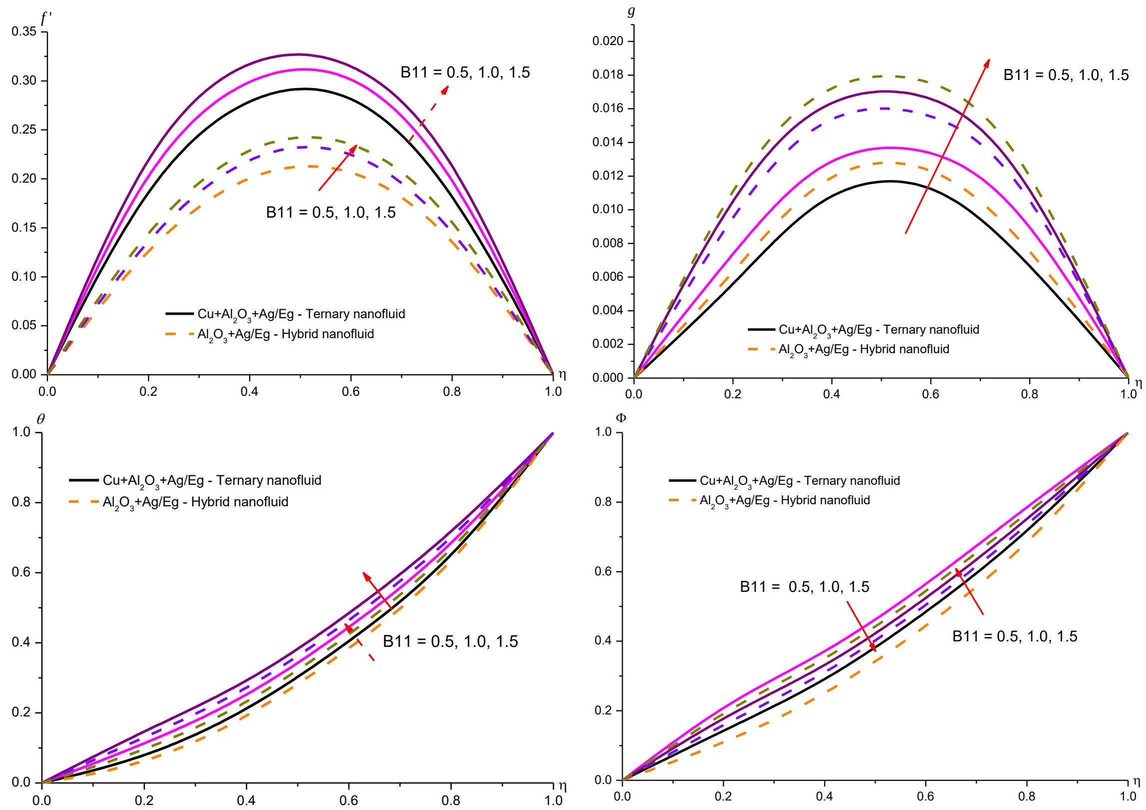

Fig.13 : Impact of B11(temperature dependent heat source parameter) on f', g, θ,Φ

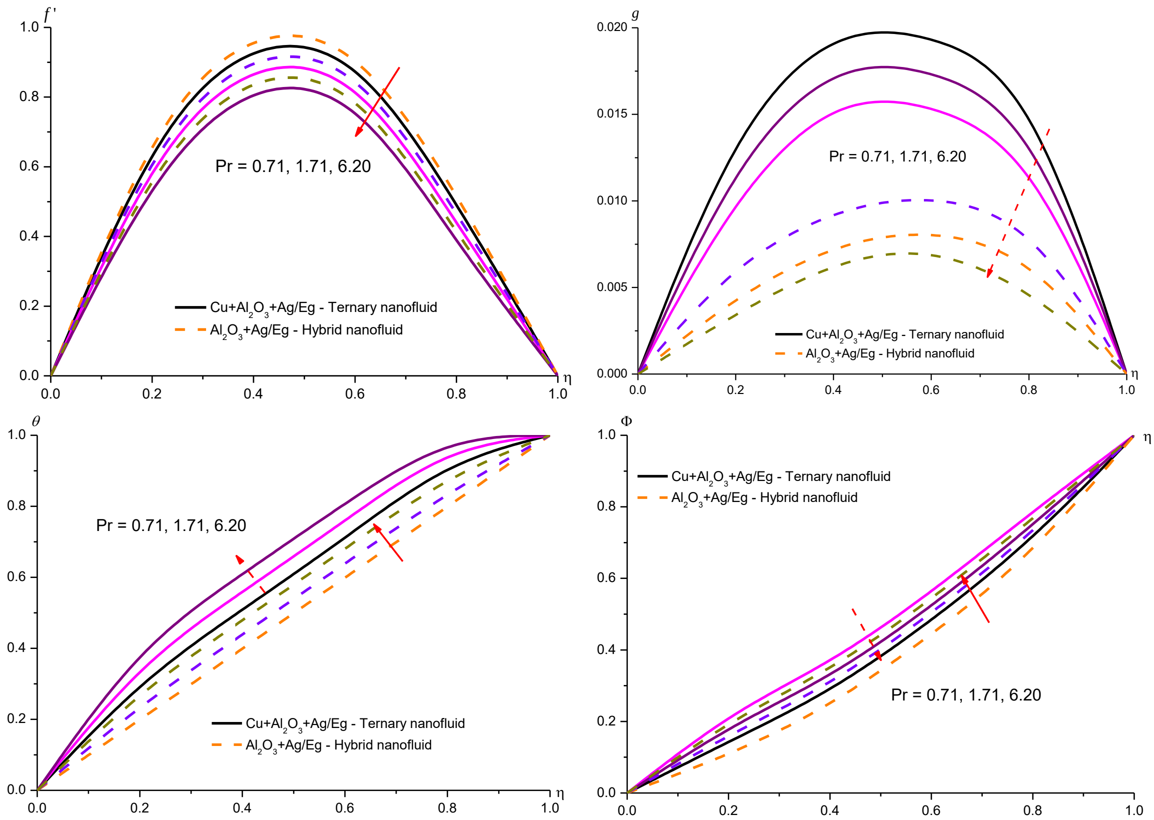

Fig.16 : Impact of Pr(Prandtl number) on f', g, θ,Φ

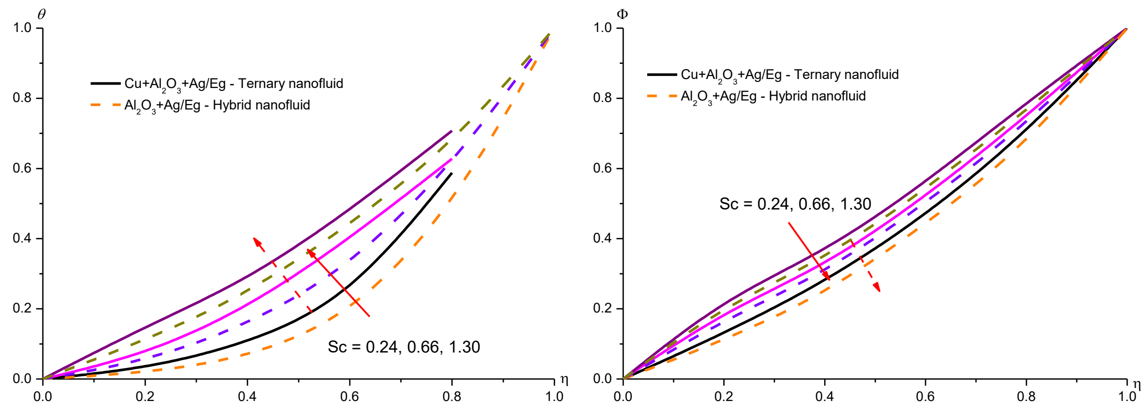

Fig.17 : Impact of Sc(Schmidt number) on f', g, θ,Φ

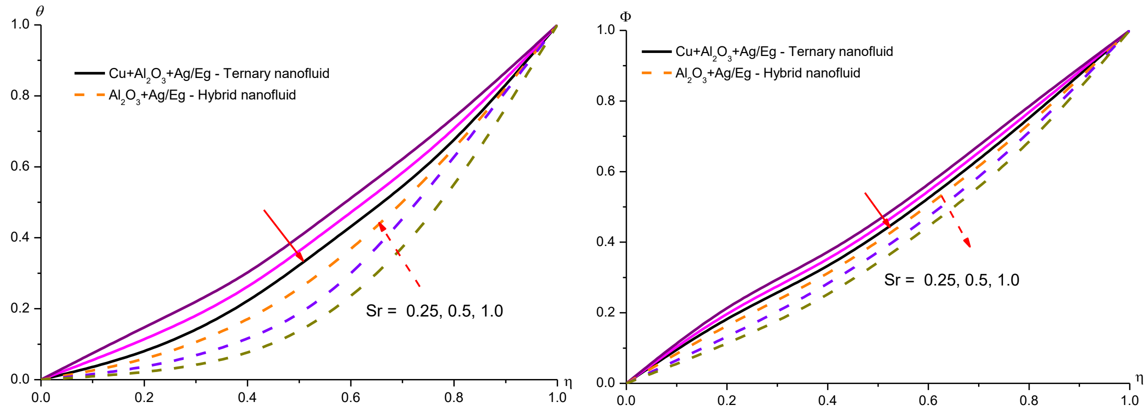

Fig.18 : Impact of Sr(Soret parameter) on f', g, θ,Φ

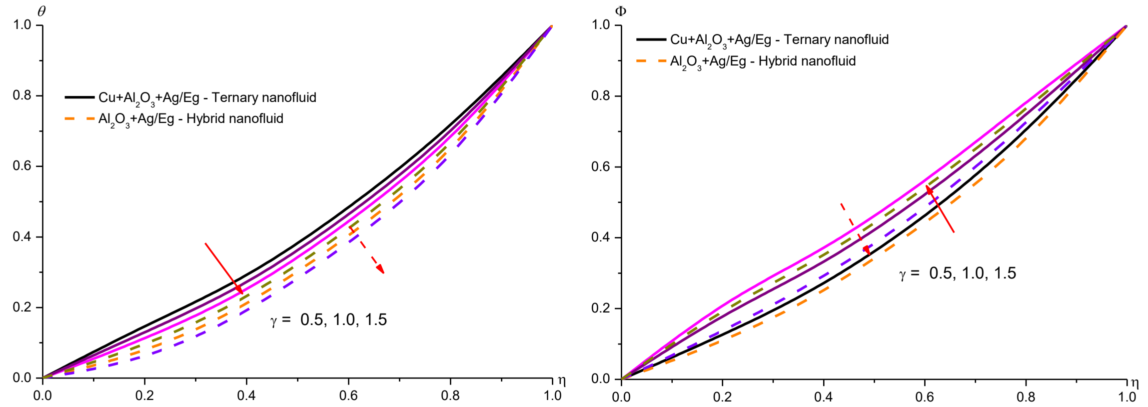

Fig.19 : Impact of γ(Chemical reaction) on f', g, θ,Φ

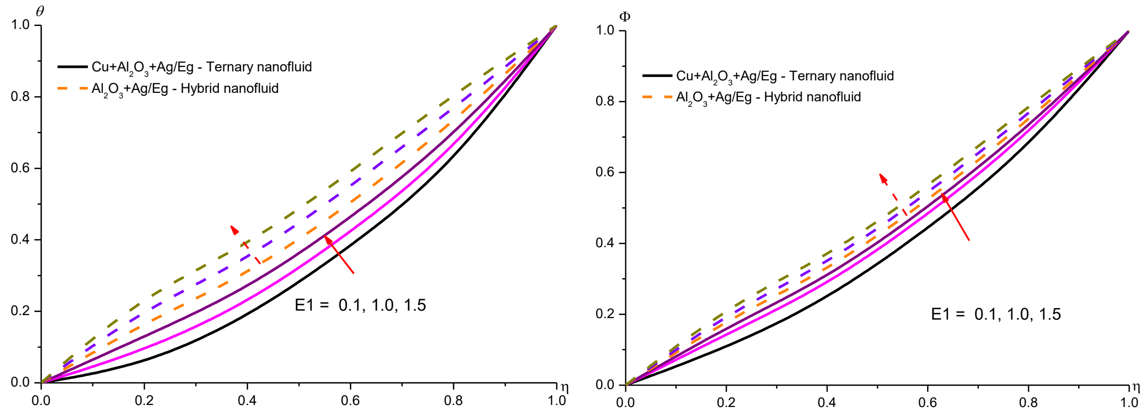

Fig.21 : Impact of E1(Activation energy) on f', g, θ,Φ

6. CONCLUSIONS:

In the present study, a numerical investigation is considered in order to demonstrate the influence of various parameters on the flow variables. The important findings of this analysis are:

1. Increase in Grashof number(G)/Space and temperature dependent heat source (A11,B11)/ Soret parameter(Sr)/Activation energy(E1) augments the axial and secondary velocities in the flow region.
2. Increase in radiation parameter(Rd) reduces both axial and secondary velocities.

3. Increase in chemical reaction parameter(γ)/enhances axial velocity(f') and decays the secondary velocity(g). Higher the nanoparticle volume fraction(ϕ)of the ternary/hybrid nanofluids reduces the axial velocity and augments the secondary velocity(g).
4. The temperature (θ) experiences enhancement with rising values of G/M/fs/Rd/ Ec/β/ Pr/Sc/Sr/γ/E1 in E based ternary and hybrid nanofluids.
5. The nanoconcentration(Φ) increases with higher values of G/K/γ/E1 and reduces with raise in ϕ/M/fs/B/β/Rd/Sc/Sr in both ternary and hybrid nanofluids.
6. The skin friction component(τx) grows with increase in ϕ/γ/E1/ while τz increases with higher values of A11,B11/Sc/Sr/γ/Pr at η=0,1 in Eg based ternary/hybrid nanofluids. Increase in Rd reduces τx,τz in Eg based ternary nanofluid and enhances in Eg base hybrid nanofluid at both the walls. Increase in squeezing parameter(β)/Eckert number(Ec) enhances τx at η=0 while at η=1,it decays in Eg based ternary/hybrid nanofluids. Increase in activation energy(E1)/Eckert number(Ec) enhances τz at η=0 in Eg based ternary nanofluid while at η=1,it reduces in ternary nanofluid,enhances in hybrid nanofluid.
7. The rate of heat transfer(Nu)enhances with increase in B11 and reduces with increase in E1/Sc/γ in both Eg based ternary/hybrid nanofluids at η=0,1.Nu decays at η=0 and enhances at η=1 in Eg based ternary nanofluid while in Eg baseed hybrid nanofluid,Nu enhances at both the walls with increase in squeezing parameter(β)/ nanoparticle volume fraction(ϕ).
8. The rate of mass transfer(Sh) enhances at η=0 and decaqys at η=1 in Eg based ternary/ hybrid nanofluids with rising values of G/β/Sc/Activation energy(E1).Increase in chemical reaction(γ) reduces Sh in Eg based ternary nanofluid at η=0,1 while in Eg baqsed hybrid nanofluid, Sh enhances at η=0, decays at η=1.Higher the Thermo-diffusion(Sr) enhances Sh at η=0,reduces at η=1 in Eg based ternary nanofluid while in Eg based hybrid nanofluid, Sh decays at both the walls.
9. The values of skin friction τz, Nu and Sh in Eg based ternary nanofluid are relatively greater than those in Eg based hybrid nanofluid at η=0,1 while opposite behaviour is noticed in the case of Skin friction component(τx) at η=0,1.

Table 2 : Variation of Skin friction ($\tau_{x,z}$), Nusselt number (Nu) and Sherwood number(Sh) at η = 0

Parameter		$Cu+Al_2O_3+Ag/Eg$ Ternary nanofluid				Al_2O_3+Ag/Eg Hybrid nanofluid			
		τx(0)	τz(0)	Nu(0)	Sh(0)	τx(0)	τz(0)	Nu(0)	Sh(0)
G	2	0.609471	0.910357	0.104609	0.947886	0.728182	1.01967	0.110984	1.04863
	4	0.560026	0.927096	0.104617	0.884606	0.696097	1.02916	0.110986	1.05286
	6	0.501421	0.946254	0.104627	0.836075	0.657686	1.04035	0.110989	2.12948
M	0.5	0.609471	0.910357	0.104609	0.947886	0.624205	0.90945	0.110984	1.05106
	1	0.660396	0.961797	0.104596	0.881804	0.684229	0.97152	0.110987	1.05305
	1.5	0.717444	1.022984	0.104581	0.829781	0.739029	1.03197	0.110992	4.29337
fs	0.1	0.609471	0.910357	0.104609	0.947886	0.624205	0.90945	0.110984	1.05106
	0.2	0.543307	1.039224	0.104615	0.884733	0.556278	1.04035	0.110985	1.05598
	0.3	0.490911	1.164944	0.104619	0.835572	0.502658	1.16803	0.110989	2.29754
Rd	0.5	0.609471	0.910357	0.104609	0.946971	0.624205	0.90945	0.110984	1.05104
	1.5	0.608895	0.914474	0.099824	0.899833	0.624215	0.90952	0.110905	1.05489

Parameter		$Cu+Al_2O_3+Ag/Eg$ Ternary nanofluid				Al_2O_3+Ag/Eg Hybrid nanofluid			
		τx(0)	τz(0)	Nu(0)	Sh(0)	τx(0)	τz(0)	Nu(0)	Sh(0)
	5	0.608646	0.916134	0.097891	0.853596	0.624219	0.90956	0.110876	1.05901
Ec	0.05	0.609471	0.910357	0.104609	0.947886	0.728182	1.01967	0.110984	1.04863
	0.1	0.609469	0.910391	0.104571	0.883295	0.728180	1.01967	0.110983	1.05204
	0.2	0.609458	0.910422	0.104535	0.832996	0.728178	1.01956	0.110980	2.29362
b	0.5	0.609471	0.910357	0.104609	0.946971	0.624205	0.90945	0.110984	1.05104
	1.5	0.580698	0.870737	0.104612	0.882977	0.595894	0.87189	0.110986	1.05511
	5.0	0.570532	0.856916	0.104616	0.832876	0.585932	0.85880	0.110988	1.05928
B	0.2	0.609471	0.910357	0.104609	0.947886	0.624205	0.90947	0.110984	1.05106
	0.4	0.608494	0.917265	0.096582	0.913714	0.624213	0.90956	0.110856	1.05521
	0.6	0.607046	0.925974	0.086502	0.893522	0.624221	0.90966	0.110728	2.30206
ϕ	0.05	0.609471	0.910357	0.104609	0.946971	0.624205	0.90945	0.110984	1.04138
	0.10	0.609476	0.910355	0.104611	1.022964	0.624208	0.90943	0.110986	1.13975
	0.12	0.609481	0.910350	0.104614	1.044534	0.624210	0.90940	0.110989	1.16537
A11	0.5	0.609471	0.910357	0.104609	0.947886	0.728180	1.01967	0.110984	1.04863
	1.0	0.609475	0.910343	0.104626	0.883085	0.728182	1.01969	0.110987	1.05203
	1.5	0.609479	0.910326	0.104645	0.832625	0.728186	1.01973	0.110993	2.29354
B11	0.5	0.609471	0.910357	0.104609	0.946971	0.624205	0.90949	0.110984	1.04138
	1.0	0.506445	0.875803	0.104606	1.107645	0.518698	0.87359	0.110987	1.24345
	1.5	0.440548	0.852146	0.104603	1.225755	0.451274	0.84885	0.110994	1.38527
Pr	0.71	0.609471	0.910357	0.104609	0.947886	0.728182	1.01967	0.110984	1.04863
	1.71	0.607967	0.920696	0.092589	0.928655	0.728216	1.01984	0.110678	1.05311
	6.20	0.605282	0.935284	0.075768	0.927774	0.728249	1.02678	0.110619	2.66303
Sc	0.24	------	------	0.104609	0.947886	------	------	0.110984	1.05106
	0.66	------	------	0.104635	2.223985	------	------	0.110985	2.82404
	1.30	------	------	0.104652	3.804957	------	------	0.101094	3.03834
Sr	0.25	------	------	0.104609	0.946971	------	------	0.110984	1.05104
	0.5	------	------	0.104607	0.883156	------	------	0.110983	1.05446
	1.0	------	------	0.104606	0.833739	------	------	0.110980	1.05842
γ	0.5	------	------	0.104609	0.946971	------	------	0.110984	1.05104
	1.0	------	------	0.104611	1.022956	------	------	0.110989	1.25566
	1.5	------	------	0.104614	1.044553	------	------	0.110995	1.40695
E1	0.1	------	------	0.104609	0.946971	------	------	0.110984	1.04138
	0.2	------	------	0.104611	1.022956	------	------	0.110986	1.13975
	0.3	------	------	0.104617	1.044553	------	------	0.110989	1.16537

7. References

1. Ahmed W., Kazi S. N., Chowdhury Z. Z.: "Heat transfergrowth of sonochemically synthesized novel mixed metaloxide ZnO+ Al2O3+ TiO2/DW based ternary hybrid nano-fluids in a square flow conduit," Renewable and SustainableEnergy Reviews, vol. 145, Article ID 111025, 2021.

2. Arif M., Kumam P., Kumam W., Khan I., Ramzan M., A fractional model of Casson fluid with ramped wall temperature: engineering applications of engine oil, Comput. Math. Methods Med. (2021) e1162.
3. Beg O.A, Mabood F and Nazrul Islam M. : Homotopy simulation of nonlinear unsteadyrotating nanofluid flow from a spinning body. *International Journal of Engineering Mathematics* 2015; Article ID 272079, 15 pages, http://dx.doi.org /10.1155/2015/272079.
4. Bhatti M. M., Khalique C. M., B´eg T. A., B´eg O. A., and Kadir A., "Numerical study of slip and radiative effects onmagnetic Fe 3 O 4-water-based nanofluid flow from a non-linear stretching sheet in porous media with Soret and Dufourdiffusion," Modern Physics Letters B, vol. 34, no. 02, Article ID2050026, 2020.
5. Buongiorno J. : Convective transport in nanofluids, ASME J. Heat Transfer, V.128, pp. 240–250(2006).
6. Choi S. U. and Eastman J. A., Enhancing thermal Conductivityof Fluids with Nanoparticles (No. ANL/MSD/CP-84938;CONF-951135-29), Argonne National Lab, IL (United States),1995.
7. Choi S.U.S., Siginer D.A., Wang H.P. : Enhancing Thermal Conductivity of Fluids with Nanoparticles, Developments and Applications of Non-Newtonian Flows, The American Society of Mechanical Engineers, New York, FED-vol. 231/MDvol. 66, pp. 99–105 (1995).
8. Cortell R., "Viscous flow and heat transfer over a nonlinearlystretching sheet," Applied Mathematics and Computation,vol. 184, no. 2, pp. 864–873, 2007.
9. Das K. : Flow and heat transfer characteristics of nanofluids in a rotating frame, Alexandria Eng. J., 53 (3), pp.757–766(2014).
10. Das K., "Nanofluid flow over a non-linear permeablestretching sheet with partial slip," Journal of the Egyptianmathematical society, vol. 23, no. 2, pp. 451–456, 2015.
11. Dezfulizadeh A., Aghaei A., Joshaghani A. H., and Najafizadeh M. M., "An experimental study on dynamicviscosity and thermal conductivity of water-Cu-SiO2-MWCNT ternary hybrid nanofluid and the development ofpractical correlations," Powder Technology, vol. 389,pp. 215–234, 2021
12. Dogonchi A. S., Hashemi-Tilehnoee M., Waqas M., Seyyedi S. M., Animasaun I. L., and Ganji D. D., "(e in-fluence of different shapes of nanoparticle on Cu–H2Onanofluids in a partially heated irregular wavy enclosure,"Physica A: Statistical Mechanics and Its Applications, vol. 540,Article ID 123034, 2020
13. Domairry, G., & Aziz, A. (2009). Approximate analysis of MHD squeeze flow between two parallel disks with suction or injection by homotopy perturbation method. Mathematical Problems in Engineering, 2009, 603916.
14. Fatunmbi E. O., Okoya S. S., and Makinde O. D., "Convectiveheat transfer analysis of hydromagnetic micropolar fluid flowpast an inclined nonlinear stretching sheet with variablethermo-physical properties," Diffusion Foundations, vol. 26,pp. 63–77, 2020.
15. Freidoonimehr N., Rostami B, Rashidi M.M., Momoniat E. : Analytical modelling of three-dimensional squeezing nanofluid flow in a rotating channel on a lower stretching porous wall, Math. Probl. Eng., 2014,14, 692728 (2014).
16. Gireesha B.J., Mahanthesh B., Gorla R.S.R. : Suspended particle effect on nanofluid boundary layer flow past a stretching surface, J. Nanofluids, V.3 (3), pp. 267–277 (2014).

17. Haider S.M.A., Ali B., Wang Q., Zhao C., Stefan blowing impacts on unsteady MHD flow of nanofluid over a stretching sheet with electric field, thermal radiation and activation energy, Coatings 11 (9) (2021) 1048.
18. Hamad M.A.A., Pop I. : Unsteady MHD free convection flow past a vertical permeable flat plate in a rotating frame of reference with constant heat source in a nanofluid, Heat Mass Transfer, V.47, pp.1517–1524 (2011).
19. Hamza, E. A. (1988). The magnetohydrodynamic squeeze film. Journal of Tribology, 110, 375–377.
20. Hayat Khursheed Muhammad, Muhammad Farooq, Ahmad Alsaedi [*] : Unsteady Squeezing Flow of Carbon Nanotubes with Convective Boundary Conditions, PLOS ONE (Squeezing Flow of Carbon Nanotubes), May 5, 2016, pp/1-17, DOI:10.1371/journal.pone.0152923.
21. Hayat T., Haider F., and Alsaedi A., "Darcy-Forchheimer flowwith nonlinear mixed convection," Applied Mathematics andMechanics, vol. 41, no. 11, pp. 1685–1696, 2020.
22. Hayat T., Imtiaz M., Alsaedi A., and Kutbi M. A., "MHDthree-dimensional flow of nanofluid with velocity slip andnonlinear thermal radiation," Journal of Magnetism andMagnetic Materials, vol. 396, pp. 31–37, 2015.
23. Hayat T., Waqas M., Shehzad S. A., and Alsaedi A., "On modelof Burgers fluid subject to magneto nanoparticles and con-vective conditions," Journal of Molecular Liquids, vol. 222,pp. 181–187, 2016.
24. Hayat, T. , Qayyum, A. and Alsaedi, A. (2015), "Three-dimensional mixed convection squeezing flow", *Applied Mathematics and Mechanics – English Edition.* , Vol. 36 No. 1, pp. 47-60.
25. Hayat, T., Yousaf, A., Mustafa, M., & Obaidat, S. (2012). MHD squeezing flow of second-grade fluid between two parallel disks. International Journal for Numerical Methods in Fluids, 69, 399–410.
26. Hong K., Alizadeh R., Ardalan M. V., "Numerical studyof nonlinear mixed convection inside stagnation-point flowover surface-reactive cylinder embedded in porous media,"Journal of 6ermal Analysis and Calorimetry, vol. 141, no. 5,pp. 1889–1903, 2020.
27. Hussain, A., Mohyud-Din, S. T., & Cheema, T. A. (2012). Analytical and numerical approaches to squeezing flow and heat transfer between two parallel disks with velocity slip and temperature jump. Chinese Physics Letters, 29, 114705.
28. Ibrahim W. and Gamachu D., "Nonlinear convection flow ofWilliamson nanofluid past a radially stretching surface," AIPAdvances, vol. 9, no. 8, Article ID 085026, 2019.
29. Joneidi, A. A., Domairry, G., & Babaelahi, M. (2010). Effect of mass transfer on a flow in the magnetohydrodynamic squeeze film between two parallel discs with one porous disk. Chemical Engineering Communications, 198, 299–311.
30. Kalpana G., Madhura K.R., Kudenatti R.B., Magnetohydrodynamic boundary layer flow of hybrid nanofluid with the thermophoresis and Brownian motion in an irregular channel: a numerical approach, Eng. Sci. Technol. an Int. J. (2021), 101075.
31. Khan A., Hassan B., Ashraf E. E., and Shah S. Y. A., "(er-mally dissipative micropolar hybrid nanofluid flow over aspinning needle influenced by Hall current and gyrotacticmicroorganisms," Heat Transfer, vol. 51, no. 1, pp. 1170–1192,2022.
32. Khan A., Saeed A., Tassaddiq A., "Bio-convective andchemically reactive hybrid nanofluid flow upon a thin stirringneedle with viscous dissipation," Scientific Reports, vol. 11,no. 1, pp. 8066–8117, 2021.

33. Khan U., Adnan B. Ullah, Abdul Wahab H., Ullah I., Almuqrin M. A., and Khan I., "Comparative thermal trans-port mechanism in Cu-H2O and Cu-Al2O3/H2O nanofluids:numerical investigation," Waves in Random and ComplexMedia, pp. 1–16, 2022.
34. Khursheed Muhammad, Hayat T., Momani S., Asghar S. [*] : FDM analysis for squeezed flow of hybrid nanofluid in presence of Cattaneo-Christov (C-C) heat flux and convective boundary condition, Alexandria Engineering Journal (2022) 61, 4719–4727, Elsevier Alexandria Engineering Journal, https://doi.org/10.1016/j.aej.2021.10.027
35. Krishna M.V., Ahammad N.A., Chamkha A.J., Radiative MHD flow of Casson hybrid nanofluid over an infinite exponentially accelerated vertical porous surface, Case Stud. Therm. Eng. 27 (2021), 101229.
36. Kuznetsov A.V., Nield D.A. : Natural convective boundary layer flow of a nanofluid past a vertical plate, Int. J. Therm. Sci. V.49, pp.243–247, (2010).
37. Leider, P. J., & Bird, R. B. (1974). Squeezing flow between parallel disks. I. Theoretical analysis. Industrial and Engineering Chemistry Fundamentals, 13, 336–341.
38. Lund L. A., Wakif A., Omar Z., Khan I., and Animasaun I. L.,"Dynamics of water conveying copper and alumina nano-materials when viscous dissipation and thermal radiation aresignificant: single-phase model with multiple solutions,"Mathematical Methods in the Applied Sciences, 2022.
39. Mahanthesh B, Gorla R S R, Gireesha B J : "Mixed convection squeezing three-dimensional flow in a rotating channel filled with nanofluid", *International Journal of Numerical Methods for Heat & Fluid flow,* V.26, Issue 5, pp.25-32(2016)
40. Makinde O. D. and Eegunjobi A. S., "MHD flow of a reactingand radiating nanoliquid past an inclined heated permeableplate: analysis of entropy generation," Latin American AppliedResearch-An international journal, vol. 51, no. 4, pp. 269–276,2021.
41. Manjunatha S., Puneeth V., Gireesha B. J., and Chamkha A.,"(eoretical study of convective heat transfer in Ternarynanofluid flowing past a stretching sheet," Journal of Appliedand Computational Mechanics, vol. 8, pp. 1279–1286, 2021.
42. Mohib Hussain, Mohib Hussain, Muhammad Imran, Hassan Waqas,*, Taseer Muhammad, Sayed M. Eldin : An efficient heat transfer analysis of MHD flow of hybrid nanofluid between two vertically rotating plates using Keller box scheme, Case Studies in Thermal Engineering 49 (2023) 103231, https://doi.org/10.1016/j.csite.2023.103231, www.elsevier.com/locate/csite
43. Mousavi, S.M.; Esmaeilzadeh, F.; Wang, X.P. Effects of temperature and particles volume concentration on the thermophysical properties and the rheological behavior of $CuO/MgO/TiO_2$ aqueous ternary hybrid nanofluid. *J. Therm. Anal. Calorim.* **2019**, *137*, 879–901.
44. Munawar, S. , Mehmood, A. and Ali, A. (2012), Three-dimensional squeezing flow in a rotating channel of lower stretching porous wall, *Computers and Mathematics with Applications* , Vol. 64 No. 6, pp. 1575-1586.
45. Mustafa, M. , Hayat, T. and Obaidat, S. (2012), On heat and mass transfer in the unsteady squeezing flow between parallel plates, *Meccanica* , Vol. 47 No. 7, pp. 1581-1589.
46. Nadeem S and Saleem S. : Unsteady mixed convection flow of nanofluid on a rotating cone with magnetic field. *Appl. Nanoscience*; V.4: pp.405-414(2014).
47. Najiyah Safwa Khashi, Iskandar Waini2, Norihan Md Arifin2* & Ioan Pop [*] have examined the unsteady squeezing flow of Cu-Al_2O_3/water hybrid nanofluid in a horizontal channel with magnetic

field, (2021) 11:14128, https://doi.org/10.1038/s41598-021-93644-4, www.nature.com/scientificreports.
48. Nimer Murshid, Hasan Mulki, Mahmoud Abu-Samha, Wahib Owhaib, S. Suresh Kumar Raju, Chakravarthula S. K. Raju , Macherla JayachandraBabu, Raad Z. Homod and Wael Al-Kouz : Entropy Generation and Statistical Analysis of MHD Hybrid Nanofluid Unsteady Squeezing Flow between Two Parallel Rotating Plates with Activation Energy, Nanomaterials 2022, 12, 2381. https://doi.org/10.3390/nano12142381, https://www.mdpi.com/journal/nanomaterials
49. Ramzan M., Khan N.S., Kumam P., Khan R., A numerical study of chemical reaction in a nanofluid flow due to rotating disk in the presence of magnetic field, Sci. Rep. 11 (1) (2021) 1–24.
50. Ramzan M., Khan N.S., Kumam P., Mechanical analysis of non-Newtonian nanofluid past a thin needle with dipole effect and entropic characteristics, Sci. Rep. 11 (1) (2021) 1–25.
51. Ramzan M., Saeed A., Kumam P., Ahmad Z., Junaid M.S., Khan D., Influences of Soret and Dufour numbers on mixed convective and chemically reactive Casson fluids flow towards an inclined flat plate, Heat Trans (2022).
52. Rana P, Bhargava R and Beg O.A. : Finite element simulation of unsteady magnetohydrodynamic transport phenomena on a stretching sheet in a rotating nanofluid. *Proc. I Mech. E- Part N: J. Nano materials, Nanoengineering and Nanosystems*, V.227: pp.77–99(2013).
53. Rasool G.and Wakif A., "Numerical spectral examination ofEMHD mixed convective flow of second-grade nanofluidtowards a vertical Riga plate using an advanced version of therevised Buongiorno's nanofluid model," Journal of 6ermalAnalysis and Calorimetry, vol. 143, no. 3, pp. 2379–2393, 2021.
54. Reddy M.V., Lakshminarayana P., Cross-diffusion and heat source effects on a three-dimensional MHD flow of Maxwell nanofluid over a stretching surface with chemical reaction, Eur. Phys. J. Spec. Top. 230 (5) (2021) 1371–1379.
55. Rooman M., Jan M. A., Shah Z., and Alzahrani M. R., "En-tropy generation and nonlinear thermal radiation analysis onaxisymmetric MHD Ellis nanofluid over a horizontally per-meable stretching cylinder," Waves in Random and ComplexMedia, pp. 1–15, 2022
56. Sadeghi M. S., Tayebi T., Dogonchi A. S., Nayak M. K., and Waqas M., "Analysis of thermal behavior of magneticbuoyancy-driven flow in ferrofluid–filled wavy enclosurefurnished with two circular cylinders," International Com-munications in Heat and Mass Transfer, vol. 120, Article ID104951, 2021.
57. Sahoo R. R., "Heat transfer and second law characteristics ofradiator with dissimilar shape nanoparticle-based ternaryhybrid nanofluid," Journal of 6ermal Analysis and Calo-rimetry, vol. 146, no. 2, pp. 827–839, 2021.
58. Sahoo, R.R.; Kumar, V. Development of a new correlation to determine the viscosity of ternary hybrid nanofluid. *Int. Commun. Heat Mass Transf.* **2019**, *111*, 104451.
59. Seyyedi S. M., Dogonchi A. S., Hashemi-Tilehnoee M., Waqas M., and Ganji, D. D. "Entropy generation and eco-nomic analyses in a nanofluid filled L-shaped enclosuresubjected to an oriented magnetic field," Applied 6ermalEngineering, vol. 168, Article ID 114789, 2020.
60. Shaban, M., Shivanian, E., & Abbasbandy, S. (2013). Analyzing magnetohydrodynamic squeezing flow between two parallel disks with suction or injection by a new hybrid method based on the Tau method and the homotopy analysis method. European Physical Journal Plus, 128, 1–10.

61. Shah N. A., Wakif A., El-Zahar E. R., umma, and Yook S. J., "Heat transfers thermodynamic activity of a sec-ond-grade ternary T.nanofluid flow over a vertical plate withAtangana-Baleanu time-fractional integral," Alexandria En-gineering Journal, vol. 61, no. 12, pp. 10045–10053, 2022.
62. Shaw S., Dogonchi A. S., Nayak M. K., and Makinde O. D.,"Impact of entropy generation and nonlinear thermal radi-ation on Darcy–Forchheimer flow of MnFe2O4-Casson/waternanofluid due to a rotating disk: application to brain dy-namics," Arabian Journal for Science and Engineering, vol. 45,no. 7, pp. 5471–5490, 2020.
63. Shaw S., Kameswaran P. K., and Sibanda P., "Effects of slip onnonlinear convection in nanofluid flow on stretching sur-faces," Boundary Value Problems, vol. 2016, no. 1, pp. 2–11,2016.
64. Sheikholeslami M, Hatami M and Ganji DD. : Nanofluid flow and heat transfer in a rotating system in the presence of a magnetic field. *J. Molecular Liquids*; V.190: pp.112–120 (2014).
65. Sheikholeslami M. and Ganji D. D., "Heat transfer of Cu-water nanofluid flow between parallel plates," Powder Tech-nology, vol. 235, pp. 873–879, 2013.
66. Sheikholeslami M., Ganji D.D. : Magnetohydrodynamic flow in a permeable channel filled with nanofluid, Sci. Iran, V.21 (1) , pp. 203–212 (2014).
67. Sheikholeslami M., Ganji D.D. : Unsteady nanofluid flow and heat transfer in presence of magnetic field considering thermal radiation, J. Braz. Soc. Mech. Sci. Eng. http://dx.doi.org/10. 1007/s40430-014-0228-x.
68. Shoaib M., Raja M.A.Z., Sabir M.T., Awais M., Islam S., Shah Z., Kumam P., Numerical analysis of 3-D MHD hybrid nanofluid over a rotational disk in presence of thermal radiation with Joule heating and viscous dissipation effects using Lobatto IIIA technique, Alex. Eng. J. 60 (4) (2021) 3605–3619.
69. Stefan M.J.: Versuch über die scheinbare Adhäsion, Sitzungsber. – Abt. II, Österr. Akad. Wiss., Math.- Naturwiss. K, 69 (1874) 713–721.
70. Sundar L. S., Chandra Mouli K. V., Said Z., and Sousa A. C. M., "Heat transfer and second law analysis ofethylene glycol-based ternary hybrid nanofluid under laminarflow," Journal of 6ermal Science and Engineering Applica-tions, vol. 13, no. 5, Article ID 051021, 2021.
71. Tassaddiq A., Impact of Cattaneo-Christov heat flux model on MHD hybrid nano-micropolar fluid flow and heat transfer with viscous and joule dissipation effects, Sci. Rep. 11 (1) (2021) 1–14.
72. Turkyilmazoglu M., Pop I. : Heat and mass transfer of unsteady natural convection flow of some nanofluids past a vertical infinite flat plate with radiation effect, Int. J. Heat Mass Transfer, V.59, pp.167–171(2013).
73. Umar Khan, Naveed Ahmed, Syed Tauseef Mohyud-Din [*] have analyzed numerical investigation for three dimensional squeezing flow of nanofluid in a rotating channel with lower stretching wall suspended by carbon nanotubes, Applied Thermal Engineering, Volume 113, 25 February 2017, Pages 1107-1117, https://doi.org/10.1016/j.applthermaleng.2016.11.104
74. Waini I., Ishak A., Pop I., Radiative and magnetohydrodynamic micropolar hybrid nanofluid flow over a shrinking sheet with Joule heating and viscous dissipation effects, Neural Comput. Appl. (2021) 1–12.
75. Wang X, Xu X, Choi S.U.S. : Thermal conductivity of nanoparticle fluid mixture, J. Thermophys. Heat Transfer, V.13, pp.474–480(1999).
76. Wankui Bu, Hui Xu, Ilyas Khan, Sheikh Irfan Ullah Khan, and Anwar Zeb [*] : Mixed convection squeezing flow of nanofluids in a rotating channel with thermal radiation, Hindawi Journal of Mathematics, Vol. 2022, Article ID 3885463,15 pages, 2025, https://doi.org/10.1155/2022/3885463.

77. Waqas M., "A study on magneto-hydrodynamic non-New-tonian thermally radiative fluid considering mixed convectionimpact towards convective stratified surface," InternationalCommunications in Heat and Mass Transfer, vol. 126, ArticleID 105262, 2021.
78. Waqas M., "Simulation of revised nanofluid model in thestagnation region of cross fluid by expanding-contractingcylinder," International Journal of Numerical Methods forHeat and Fluid Flow, vol. 30, no. 4, pp. 2193–2205, 2019.
79. Waqas M., Dogonchi A. S., Shehzad S. A., Khan M. I., Hayat T., and Alsaedi A., "Nonlinear convection and jouleheating impacts in magneto-thixotropic nanofluid stratifiedflow by convectively heated variable thicked surface," Journalof Molecular Liquids, vol. 300, Article ID 111945, 2020.
80. Waqas M., Hayat T., and Alsaedi A., "A theoretical analysis ofSWCNT-MWCNT and H2O nanofluids considering Dar-cy–Forchheimer relation," Applied Nanoscience, vol. 9, no. 5,pp. 1183–1191, 2019.
81. Waseem M., Gul T., Khan I., "Gravity-driven hydro-magnetic flow of couple stress hybrid nanofluid with ho-mogenous-heterogeneous reactions," Scientific Reports,vol. 11, no. 1, pp. 17498–17512, 2021